Molecular Therapy
Original Article

A self-amplifying mRNA SARS-CoV-2 vaccine candidate induces safe and robust protective immunity in preclinical models

Giulietta Maruggi,[1] Corey P. Mallett,[1] Jason W. Westerbeck,[1] Tiffany Chen,[1] Giuseppe Lofano,[1] Kristian Friedrich,[1] Lin Qu,[1,8] Jennifer Tong Sun,[1] Josie McAuliffe,[1] Amey Kanitkar,[1] Kathryn T. Arrildt,[1,9] Kai-Fen Wang,[1] Ian McBee,[1,10] Deborah McCoy,[3] Rebecca Terry,[2] Alison Rowles,[2] Maia Araujo Abrahim,[4] Michael A. Ringenberg,[3] Malcolm J. Gains,[4] Catherine Spickler,[4] Xuping Xie,[7] Jing Zou,[7] Pei-Yong Shi,[7] Taru Dutt,[5] Marcela Henao-Tamayo,[5] Izabela Ragan,[6] Richard A. Bowen,[6] Russell Johnson,[1,11] Sandra Nuti,[1] Kate Luisi,[1] Jeffrey B. Ulmer,[1] Ann-Muriel Steff,[1] Rashmi Jalah,[1] Sylvie Bertholet,[1] Alan H. Stokes,[3] and Dong Yu[1,12]

[1]GSK, Rockville, MD 20850, USA; [2]GSK, Ware, Hertfordshire SG12 ODP, UK; [3]GSK, Upper Providence, PA 19426, USA; [4]Charles River Laboratories, Laval, QC H7V 4B3, Canada; [5]Department of Microbiology, Immunology, and Pathology, Colorado State University, Fort Collins, CO 80521, USA; [6]Department of Biomedical Sciences, Colorado State University, Fort Collins, CO 80521, USA; [7]Depatment of Biochemistry and Molecular Biology, University of Texas Medical Branch, Galveston, TX 77555, USA

RNA vaccines have demonstrated efficacy against SARS-CoV-2 in humans, and the technology is being leveraged for rapid emergency response. In this report, we assessed immunogenicity and, for the first time, toxicity, biodistribution, and protective efficacy in preclinical models of a two-dose self-amplifying messenger RNA (SAM) vaccine, encoding a prefusion-stabilized spike antigen of SARS-CoV-2 Wuhan-Hu-1 strain and delivered by lipid nanoparticles (LNPs). In mice, one immunization with the SAM vaccine elicited a robust spike-specific antibody response, which was further boosted by a second immunization, and effectively neutralized the matched SARS-CoV-2 Wuhan strain as well as B.1.1.7 (Alpha), B.1.351 (Beta) and B.1.617.2 (Delta) variants. High frequencies of spike-specific germinal center B, Th0/Th1 CD4, and CD8 T cell responses were observed in mice. Local tolerance, potential systemic toxicity, and biodistribution of the vaccine were characterized in rats. In hamsters, the vaccine candidate was well-tolerated, markedly reduced viral load in the upper and lower airways, and protected animals against disease in a dose-dependent manner, with no evidence of disease enhancement following SARS-CoV-2 challenge. Therefore, the SARS-CoV-2 SAM (LNP) vaccine candidate has a favorable safety profile, elicits robust protective immune responses against multiple SARS-CoV-2 variants, and has been advanced to phase 1 clinical evaluation (NCT04758962).

INTRODUCTION

On March 11th, 2020, the World Health Organization declared the coronavirus disease 2019 (COVID-19) outbreak, caused by a novel coronavirus termed SARS-CoV-2, a global pandemic. Multifactorial approaches, including vaccines and therapeutics, have been developed to contain the devastating impact of the COVID-19 pandemic in the last 18 months.[1] In less than 2 years, an unprecedented number of vaccine candidates have been developed, with over 100 currently undergoing clinical evaluation and a few approved for emergency use or fully licensed.[2] Given the need to produce billions of doses to immunize the world's population, the unknown duration of protection in most vulnerable populations, and the need to address continuously emerging variants, more than one type of vaccine will be needed. The first SARS-CoV-2 vaccine receiving emergency use authorization in several countries and later full approval in the US is a conventional optimized non-amplifying messenger RNA (mRNA)-based vaccine, validating the mRNA vaccine platforms for rapid vaccine development.[3,4] The utility of the mRNA platform for rapid pandemic response was first reported in preclinical models in 2013 using a self-amplifying mRNA (SAM).[5]

SAM is a synthetic mRNA vaccine platform using a self-amplifying mRNA derived from an alphavirus genome.[6] SAM encodes the antigen of interest and the viral replication machinery required for intracellular RNA amplification. Unlike conventional mRNA vaccines, which only encode the antigen of interest and are translated directly

Received 20 October 2021; accepted 2 January 2022;
https://doi.org/10.1016/j.ymthe.2022.01.001.

[8]Present address: Venatorx Pharmaceuticals, Inc., Malvern, PA, USA

[9]Present address: Lawrence Livermore National Laboratory, Livermore, CA 94550, USA

[10]Present address: Novavax, Gaithersburg, MD 20878, USA

[11]Present address: RVAC Medicines, Medford, MA 02155, USA

[12]Present address: Dynavax Technologies, Emeryville, CA 94608, USA

Correspondence: Giulietta Maruggi, GSK, Rockville, MD 20850, USA.
E-mail: giulietta.x.maruggi@gsk.com
Correspondence: Dong Yu, GSK, Rockville, MD 20850, USA.
E-mail: dyu@dynavax.com

from the incoming RNA molecules, SAM can generate many copies of the mRNA in the target cell, leading to high and prolonged expression of the antigen and additional self-adjuvanting of innate immune responses.[6,7] As a result, SAM vaccines can elicit protective immune responses at lower doses,[8] possibly even with a single-dose regimen,[9–11] so they could represent an important platform for vaccine development to control the global spread of SARS-CoV-2.

SARS-CoV-2 is an enveloped, single-stranded positive-sense RNA virus in the Coronaviridae family. It carries an approximately 30,000-nucleotide genome that encodes open reading frames of four major structural proteins: spike (S), envelope, membrane, and nucleocapsid.[12] The trimeric spike glycoprotein is located on the viral surface playing an essential role in virus entry and intercellular spread and is also the major target for virus neutralizing antibodies.[13] The spike protein is a class I fusion protein, consisting of S1 and S2 domains, and exists in a metastable prefusion conformation. The prefusion spike protein binds to the human angiotensin-converting enzyme 2 (hACE2) receptor, and enter the cells via fusion of viral and host cell membranes through spike structural rearrangements,[14] or via clathrin-mediated endocytosis.[15] Introduction of two proline mutations in the C-terminal S2 fusion domain stabilizes the protein in a prefusion conformation, which exposes the receptor-binding sites and a dense cluster of neutralizing epitopes,[16] making it a prime vaccine candidate for SARS-CoV-2. For an effective and safe COVID-19 vaccine, type 1 helper (Th1) T cell responses are also highly desirable, in addition to neutralizing antibodies against the spike protein. SARS vaccines driving Th2 responses have been previously associated with enhanced lung immunopathology after challenge with SARS-CoV.[17,18]

In this paper, we report a comprehensive preclinical development of a lipid nanoparticle (LNP)-formulated SAM vaccine encoding the prefusion-stabilized SARS-CoV-2 spike full-length antigen. We assessed protective efficacy, immunogenicity, toxicity, and biodistribution of this candidate vaccine in mice, rats, and hamsters. Our results demonstrated that the SARS-CoV-2 SAM (LNP) vaccine has a favorable safety profile and elicits robust immune responses against the original SARS-CoV-2 Wuhan strain, B.1.1.7 (Alpha), B.1.351 (Beta), and B.1.617.2 (Delta) variants, supporting its current evaluation in a first-in-human phase 1 clinical trial (NCT04758962).

RESULTS

Vaccine design and characterization

To generate the SARS-CoV-2 SAM vaccine candidate, the full-length, codon-optimized spike protein (Wuhan-Hu-1 isolate), stabilized in the prefusion conformation by substitution of residues 986 and 987 with proline and substitution of the furin cleavage site with a "glycine-serine-alanine-serine" (GSAS) sequence[16] ($spike_{FL\text{-}2P}$), was cloned in an alphavirus-derived SAM vector (Figure 1A). SAM encoding green fluorescent protein or a SAM encoding unmodified wild-type spike protein ($spike_{FL}$) were used as controls. RNAs were transcribed *in vitro* from template DNA constructs using T7 polymerase, and RNA integrity was validated by agarose gel electrophoresis (Figure S1A). To assess the ability of the RNA to self-amplify, defined as potency, we measured the presence of double-stranded RNA (dsRNA) amplifying intermediates in electroporated baby hamster kidney (BHK) cells by flow cytometry using an anti-dsRNA antibody. This antibody specifically recognizes dsRNA intermediates of amplification, but not any RNA secondary structures or *in vitro*-transcribed byproducts in transfection assay (data not shown). $Spike_{FL\text{-}2P}$ SAM showed a potency, calculated as the percentage of dsRNA-positive cells, greater than 20% and 60%, with 0.1- and 1-μg RNA doses respectively (Figure S1B). Mean fluorescence intensity of positive cells was comparable to the controls, suggesting efficient self-amplification (Figure S1C). Spike intracellular expression was confirmed by flow cytometry and by immunoblot analysis using an anti-S2 antibody (Figures 1B and 1C).

Mouse myoblast C2C12 cells were transfected with SARS-CoV-2 SAM by electroporation to confirm the cellular localization of the expressed $spike_{FL\text{-}2P}$ protein in a cell type similar to the muscle cells present at the site of injection. The $spike_{FL\text{-}2P}$ protein localized on the surface of transfected cells, as measured by flow cytometry, suggesting an efficient transport of the antigen to the cell membrane (Figure 1D). Importantly, the surface-expressed $spike_{FL\text{-}2P}$ protein directly bound to the target hACE2 receptor, as shown by flow cytometry of live, unpermeabilized transfected cells incubated with soluble hACE2 and stained with an anti-ACE2 antibody (Figure 1E). Incubation with a Golgi-mediated protein transport inhibitor such as brefeldin A (BFA) substantially reduced surface expression of the spike proteins and its binding to the soluble hACE2 receptor. Therefore, the $spike_{FL\text{-}2P}$ expressed from SAM was antigenically functional, and consequently the SAM encoding $spike_{FL\text{-}2P}$ was formulated with LNP for further evaluation in animal studies.

Immunogenicity of the SARS-CoV-2 SAM (LNP) candidate vaccine in BALB/c mice

To evaluate vaccine immunogenicity in BALB/c mice, spike-specific serum antibodies as well as B and T cell responses were characterized after one or two intramuscular (i.m.) injections of SARS-CoV-2 SAM (LNP), given 3 weeks apart, at doses of 0.015 μg, 0.15 μg, or 1.5 μg, or injection of saline as a mock control (Figure S2A).

SARS-CoV-2 spike-specific serum antibodies induced by the SARS-CoV-2 SAM (LNP) vaccine candidate were measured 3 weeks after the first vaccination (3wp1, day 21) and 2 weeks after the second vaccination (2wp2, day 35). A single immunization induced high titers of anti-spike-IgG binding antibodies in a dose-dependent manner, which were further boosted after the second vaccination (Figure S2B). The neutralizing activity was measured by a vesicular stomatitis virus (VSV)-based SARS-CoV-2 (Wuhan strain) pseudovirus neutralization assay on day 21 and day 35. At all three doses (0.015 μg, 0.15 μg, and 1.5 μg), the SAM vaccine candidate induced neutralizing antibody titers after the first immunization, which were then boosted ~30-fold by the second immunization (Figure 2A). There was a clear and statistically significant dose response in antibody levels elicited by different SAM vaccine dosage levels

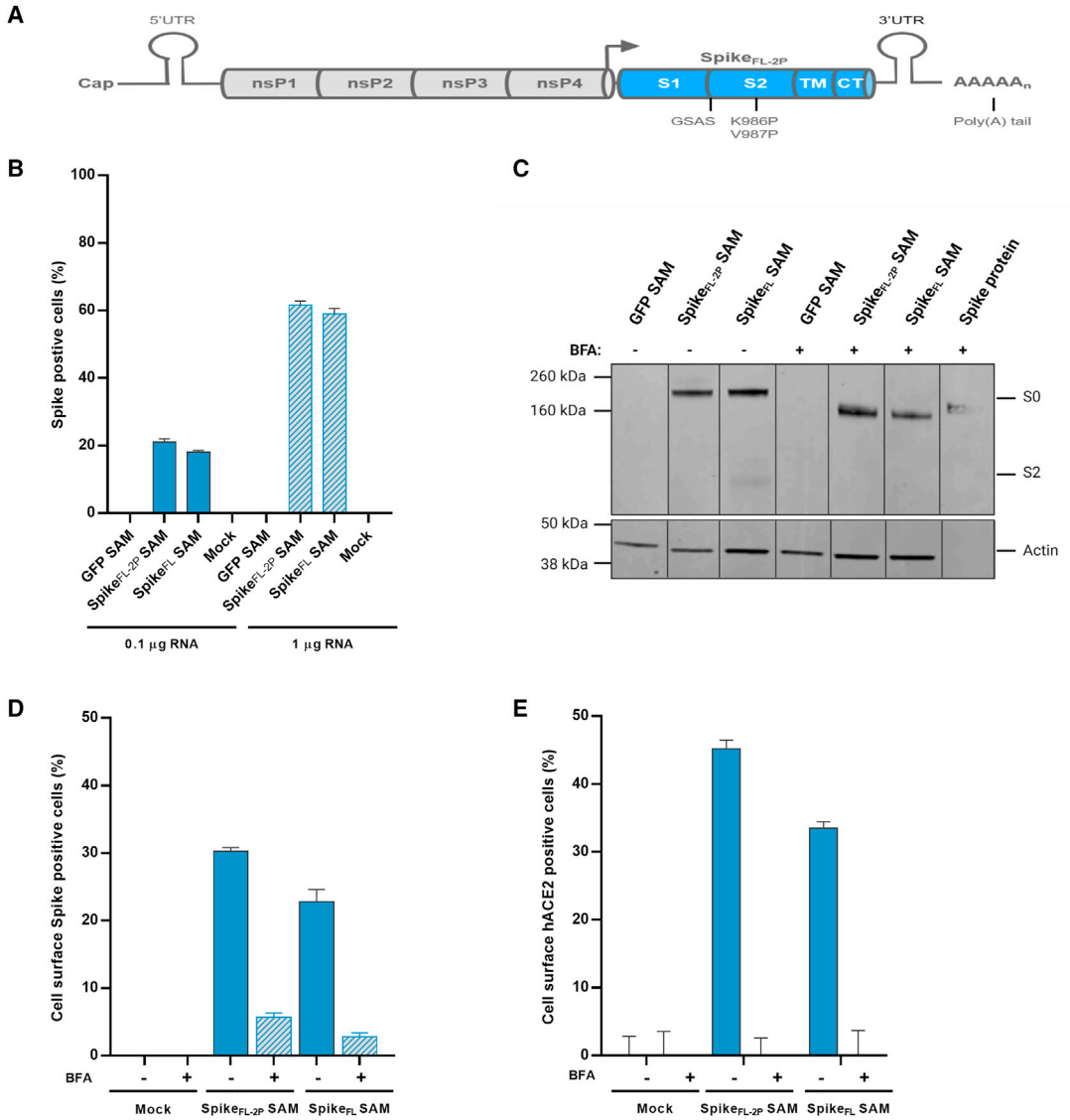

Figure 1. Vaccine design and antigen characterization

(A) Schematic representation of the SAM vector encoding the prefusion-stabilized SARS-CoV-2 spike (spike$_{FL-2P}$) protein (i.e., SARS-CoV-2 SAM). S1, S2, transmembrane (TM), and cytoplasmic (CT) domains, K986P, V987P, and GSAS mutations are indicated. (B) Percentage of spike-positive cells measured by intracellular flow cytometry 18 h after green fluorescent protein (GFP), prefusion-stabilized (spike$_{FL-2P}$), or wild-type (spike$_{FL}$) spike sequence SAM RNA electroporation of BHK cells, and intracellular staining with an anti-S2-specific antibody. (C) SAM-transfected BHK cells were also treated with (+) or without (–) BFA, and 18 h later, cell lysates were collected and analyzed by immunoblotting using anti-S2 or anti-actin antibodies. A recombinant spike protein was loaded as control. In addition, mouse C2C12 cells were transfected with SAM, treated with (+) or without (–) BFA, collected 18 h later, and surface-expressed spike protein was detected by flow cytometry using either the anti-S2-antibody (D) or incubated with soluble hACE2 and stained with an anti-hACE2 antibody (E). nsPs, non-structural proteins; UTR, untranslated regions; arrow, subgenomic promoter; kDa, kilodalton; S0, furin uncleaved full-length spike protein; S2, furin cleaved domain. Error bars represent SD of duplicate samples. Data shown are representative of at least two experiments.

($p < 0.0001$). This robust, dose-dependent neutralizing antibody response was also confirmed by a SARS-CoV-2 live virus assay (VNT_{50}, live virus 50% neutralization titers)[19] (Figure 2B). Importantly, both pseudovirus and live virus-based neutralization geometric mean titers (GMTs) following the second vaccination at all three dose levels were greater than the GMT of COVID-19 convalescent human sera (~100-fold at the 1.5 μg SAM dose) (Figures 2A and 2B). There was a strong correlation ($r = 0.7803$, $p < 0.001$) between the two neutralization assays ($pVNT_{50}$ [pseudovirus 50% neutralization titer] and VNT_{50}), indicating that the two assays were comparable in terms of measuring neutralizing antibody titers (Figure S2C).

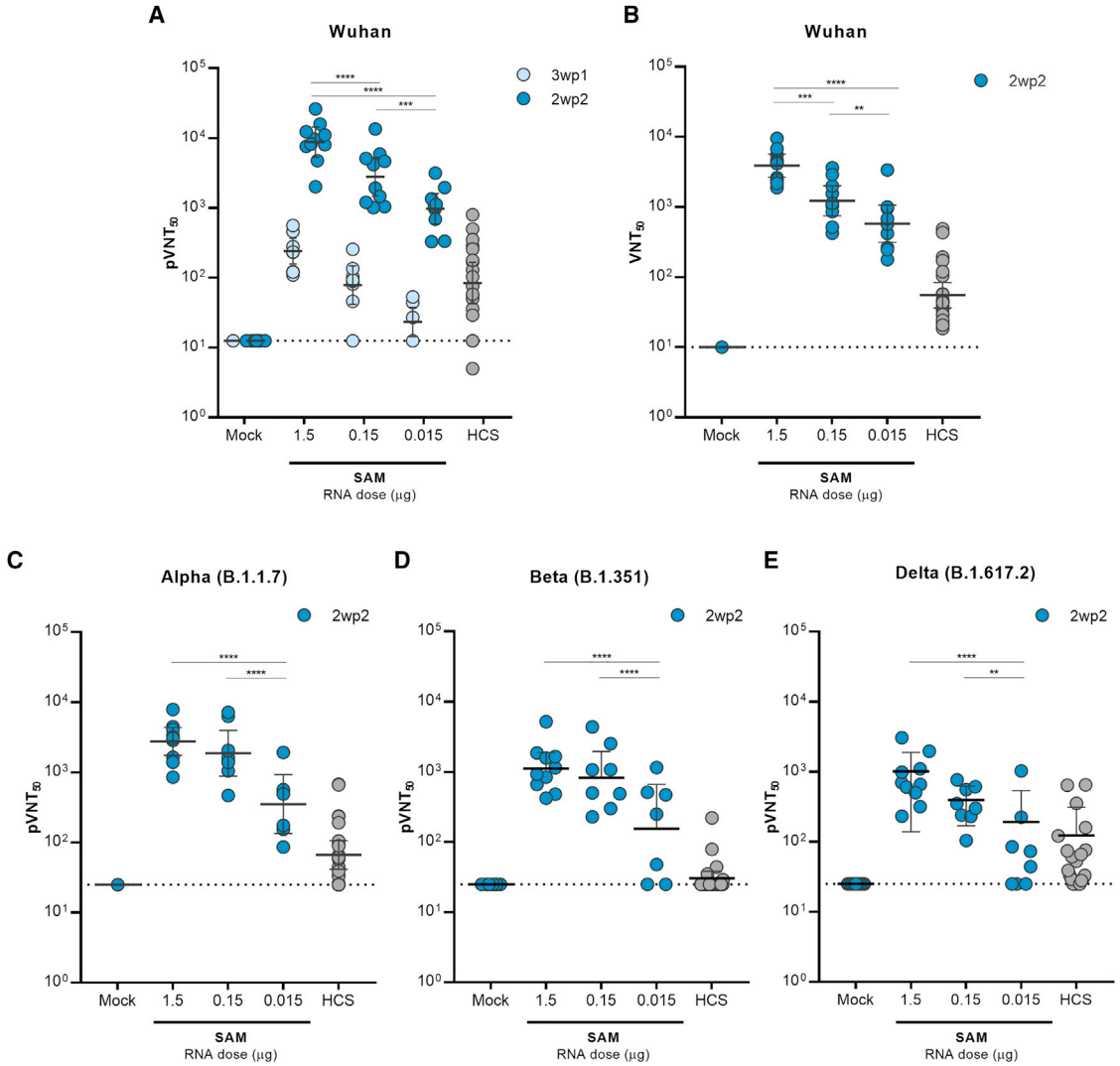

Figure 2. Humoral responses elicited by SARS-CoV-2 SAM (LNP) vaccine in mice

Pseudovirus-based spike 50% neutralization titers ($pVNT_{50}$) of immunized mice sera or human COVID-19 convalescent sera (HCS) against Wuhan (A), Alpha (B.1.1.7) (C), Beta (B.1.351) (D), or Delta (B.1.617.2) (E) spike sequences. A panel of 22 HCS was tested against Wuhan, Alpha, and Beta, whereas a panel of 21 HCS (same panel minus one subject) was tested against Delta. Mouse sera were collected 3 weeks after the first vaccination (3wp1) and 2 weeks after the second vaccination (2wp2). (B) SARS-CoV-2 50% virus neutralization titers (VNT_{50}) measured with a mNeonGreen reporter virus-based assay in sera collected 2wp2 from immunized mice or in a panel of COVID-19 HCS (n = 22). The dotted line indicates the limit of detection. Geometric means of each group ±95% confidence interval are shown. Each dot represents individual samples. Bars under p value asterisks indicate significantly different groups comparisons with **, $p < 0.01$; ***, $p < 0.001$; ****, $p < 0.0001$.

In addition to the SARS-CoV-2 Wuhan strain, 2wp2 sera from SAM-immunized mice were also tested against the Alpha (B.1.1.7), Beta (B.1.351), and Delta (B.1.617.2) variants of concern[20] using a $pVNT_{50}$ assay. GMTs of neutralization activity of mouse sera against B.1.1.7, B.1.351, and B.1.617.2 variants were reduced ($p < 0.01$) compared with the GMTs of the Wuhan strain (Figures 2C–2E). However, compared with the GMT of human convalescent sera, GMTs elicited by the SAM vaccine candidate at a dose of 0.015 μg, 0.15 μg, or 1.5 μg were 5.5-, 28-, or 40-fold higher against B.1.1.7, 5.4-, 27-, or 37-fold higher against B.1.351, and 2-, 3.2-, or 10-fold higher against B.1.617.2, respectively. This result further demonstrates that in mice the SAM vaccine candidate elicited robust immunity in both magnitude and breadth.

As the quality and longevity of humoral immune responses elicited by a vaccine rely on the generation of memory B cells,[21] we used multiparametric flow cytometry to determine the magnitude and quality of germinal center (GC) and memory B cells in draining lymph nodes (to evaluate the principal B cell immune compartment for priming) (Figures S3A–S3C) and spleens (to evaluate systemic effects of the vaccine) (Figures S3D–S3F) from immunized mice at 2wp2. Dose-dependent frequencies of spike-specific $IgD^{-}IgM^{-}$ class-switched B

cell (identified as $CD3^{-}CD19^{+}IgM^{-}IgD^{-}spike^{+}$) were observed at 1.5 and 0.15 μg SAM doses in the draining inguinal lymph nodes (Figure S3A) and spleens (Figure S3D) of immunized mice. Higher frequencies of spike-specific B cells were observed in the draining lymph nodes that consisted predominantly (over 80% in the 1.5 and 0.15 μg dose groups) of spike-specific GC B cells (identified as live $CD3^{-}CD19^{+}IgM^{-}IgD^{-}spike^{+}GL7^{+}CD95^{+}$cells) (Figure S3B). Conversely, in the spleens, most of the spike-specific B cells from SAM vaccinated groups had a memory phenotype (identified as live $CD3^{-}CD19^{+}IgM^{-}IgD^{-}spike^{+}CD95^{-}CD38^{+}$ cells) (Figure S3F), with a minimal GC phenotype (Figure S3E), indicating maturation and trafficking of spike-specific GC B cells from lymph nodes into systemic circulation to generate spike-specific memory B cells. Low and highly variable B cell responses were observed in the 0.015 μg dose group, possibly because of the very low dose used.

Further, vaccine-induced T cell-mediated immune responses against the spike antigen were analyzed in mice spleens at 2wp2 by intracellular-cytokine-staining and multi-parametric flow cytometry, after *ex vivo* restimulation with full-length spike, S1, S2, or receptor-binding domain (RBD) peptide mixes (Figures 3 and S4). The analysis measured the frequencies of total spike-specific $CD4^{+}$ and $CD8^{+}$ T cells, as well as the phenotype of various polyfunctional T cell subsets within the spike-specific $CD4^{+}$ (Th0, Th1, Th2, or Th17) and $CD8^{+}$ (Tc0, Tc1, Tc2, and Tc17 T-cytotoxic [Tc]) compartments. The SARS-CoV-2 SAM (LNP) vaccine induced robust dose-dependent total spike-specific cytotoxic $CD8^{+}$ and Th1 $CD4^{+}$ T cell responses even at the very low dose of 0.015 μg RNA (Figures 3A and 3B). The $CD8^{+}$ responses were higher than $CD4^{+}$ responses and were characterized by high expression of CD107a degranulation marker, interferon-γ (IFN-γ), tumor necrosis factor alpha (TNF-α), and interleukin-2 (IL-2) cytokines (Figure S4A) with a polyfunctional cytotoxic Tc1/Tc0 phenotype (Figure 3A) consisting primarily of $CD107a^{+}IFN\text{-}\gamma^{+}TNF\text{-}\alpha^{+}$ triple-positive and $CD107a^{+}IFN\text{-}\gamma^{+}$ double-positive $CD8^{+}$ T cells (Figure 3C) at all doses. The $CD4^{+}$ responses were characterized by expression of IFN-γ, TNF-α, and IL-2 cytokines (Figure S4B) as triple-positive or various double-positive polyfunctional combinations (Figure 3D), giving predominantly a Th1/Th0 $CD4^{+}$ T helper phenotype at all doses (Figure 3B). The IL-4/IL-13 (Th2) and IL-17F (Th17) cytokine responses were negligible in both $CD4^{+}$ and $CD8^{+}$ compartments (Figures 3 and S4). The majority of the spike-specific total $CD8^{+}$ T cell responses were detected against the S1 domain with relatively lower levels of $CD8^{+}$ responses to the S2 and RBD domains (Figure S4C), whereas similar levels of spike-specific $CD4^{+}$ responses to S1 and S2 domains with some RBD-specific $CD4^{+}$ responses were induced (Figure S4D).

Overall, these data indicate a strong induction of SARS-CoV-2 anti-spike IgG binding and broadly neutralizing antibody titers, systemic polyfunctional cytotoxic $CD8^{+}$ cell response, and Th1-driven $CD4^{+}$ T cell response by the SARS-CoV-2 SAM (LNP) vaccine candidate in mice. The polarized T cell phenotype is particularly critical for the development of a safe vaccine against SARS-CoV-2, given the potential risk of enhanced lung immunopathology associated with Th2 responses observed after coronavirus vaccine administration in animal models.[17,18]

Immunogenicity, protective efficacy, and enhanced respiratory disease assessments of SARS-CoV-2 SAM (LNP) candidate vaccine in Golden Syrian hamsters

To determine protective efficacy of the SAM vaccine candidate against SARS-CoV-2 infection, we measured clinical and virologic endpoints of SARS-CoV-2 infection in Golden Syrian hamsters after vaccination and then followed by viral challenge. Hamsters are susceptible to SARS-CoV-2, given the homology between hamster and human ACE2 receptors, supporting high levels of virus replication and transmission and leading to weight loss and severe pneumonia similar to COVID-19 patients.[22,23]

The SARS-CoV-2 SAM (LNP) vaccine candidate was injected i.m. into hamsters at a dose of 0.03 μg (low dose) or 3 μg (high dose) on day 0 and day 21; saline was used as a mock control (Figure S5A). Serum neutralizing antibody titers, measured by a plaque reduction neutralization test (PRNT90), were readily detected at 3wp1 in all the SAM vaccinated animals (Figure S5B). After the second immunization, titers were boosted significantly in both vaccinated groups ($p \leq 0.0178$). For the low dose vaccine, neutralizing antibody titers were generally higher in female than in male hamsters after both immunizations, whereas with the high dose vaccine, both genders responded comparably after both immunizations.

Three weeks after the second dose, animals in all treatment groups were challenged intranasally with 10^{4} plaque-forming units (PFU) of SARS-CoV-2 (isolate USA-WA1/2020). Oral-pharyngeal swabs were taken at 1, 2, 3, and 7 days post infection (dpi) and assayed by plaque assay to monitor viral load in the upper respiratory tract. At 1 dpi, infectious virus was detected in all groups, but viral loads in the SAM high- and low-dose groups were 156-fold and 49-fold (female hamsters) or 149-fold and 3-fold (male hamsters) lower than those in the mock control (Figures 4A and 4B). Interestingly, at 1 dpi, viral loads in male hamsters were 50-fold higher than those in female hamsters in the SAM low-dose group (Figures 4A and 4B), possibly due to the lower neutralizing antibody titers elicited in males (Figure S5B). At 3 dpi, viral loads were reduced in all SAM groups compared with mock vaccinated animals ($p < 0.0002$), approaching the limit of detection of the assay. No virus was detected at 7 dpi in SAM and mock vaccinated animals.

At 3 dpi, eight animals from each group (four female and four male hamsters) were euthanized to measure the viral loads in nasal turbinates and cranial right and caudal right lung lobes. In nasal turbinates, a vaccine dose-dependent reduction in viral load was apparent in SAM vaccinated groups. At 0.03 μg dose, the SAM vaccine reduced viral loads by 1,000-fold, but only in female hamsters (Figure 4C). At 3 μg dose, there was no detectable virus in either female or male vaccinated animals. In the cranial and lung lobes, SAM vaccine at either dose markedly reduced levels of virus ($p < 0.001$), with no detectable virus in four of the eight animals from the 0.03-μg SAM group and in all animals from the 3 μg SAM group (Figures 4D and 4E).

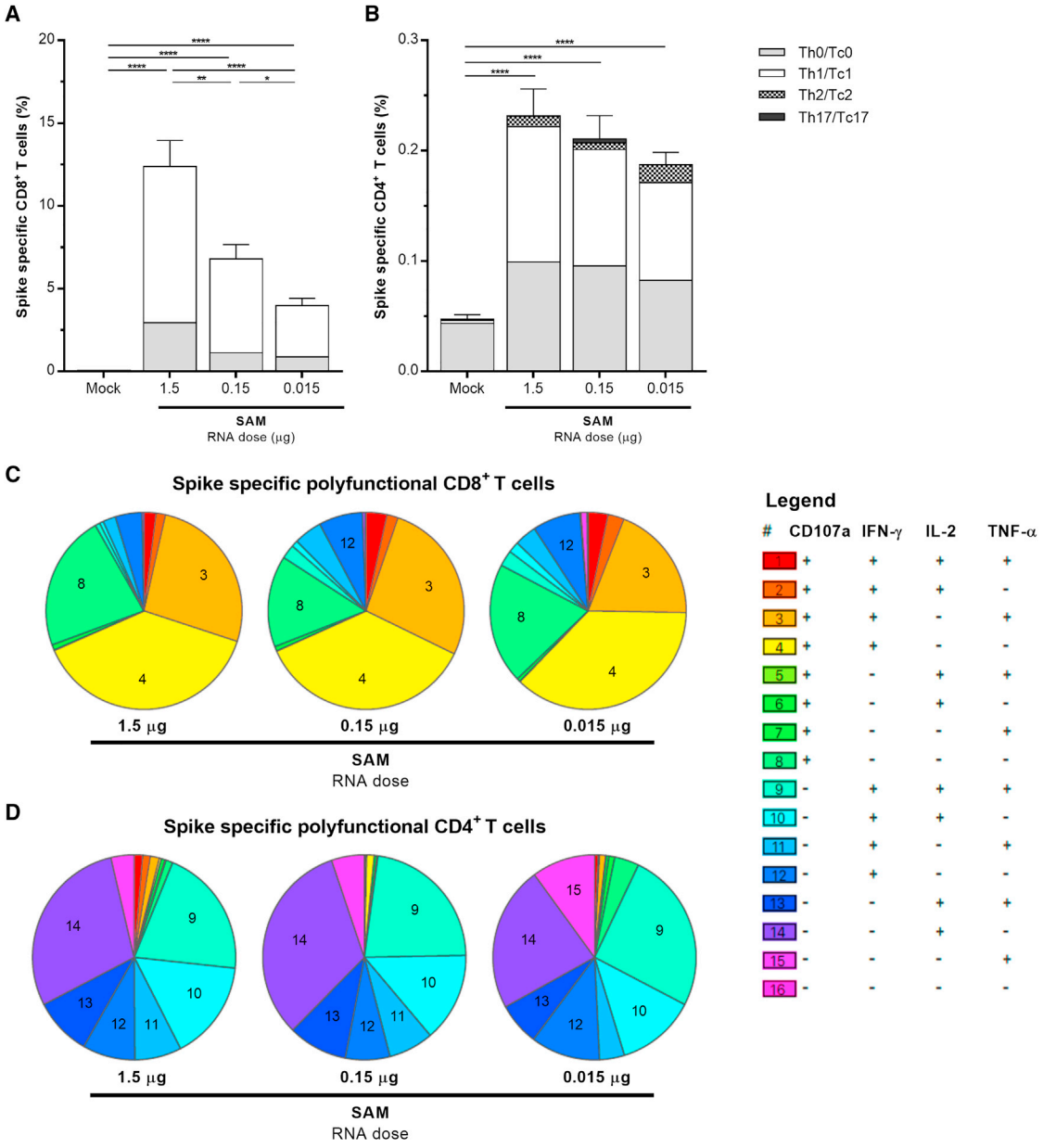

Figure 3. Cellular responses elicited by SARS-CoV-2 SAM (LNP) vaccine in mice

Splenocytes of BALB/c mice (n = 5) immunized i.m. with SAM vaccine or saline control (mock) were harvested at 2wp2, stimulated *ex vivo* with a peptide mix specific to spike$_{FL\text{-}2P}$, and analyzed for CD8$^+$ (A and C) and CD4$^+$ (B and D) T cell responses by flow cytometry. The stacked bars (A and B) indicate distribution of the Tc0/Tc1/Tc2/Tc17 cytotoxic cells within the total CD8$^+$ and the Th0/Th1/Th2/Th17 T helper cells within the CD4$^+$ spike-specific T cells (mean ± SEM). Boolean combinations for spike-specific CD8$^+$ and CD4$^+$ T cell cytokines from splenocytes of individual immunized mice were background subtracted using Pestle software, and pies were generated using SPICE software (C and D). Each pie slice represents a proportion of the total spike-specific CD8$^+$ or CD4$^+$ T cell responses for a unique sub-population comprising CD107a, IFN-γ, IL-2, or TNF-α, as indicated in the legend. Bars under p value asterisks indicate significantly different group comparisons with *, $p < 0.05$; **, $p < 0.01$; ***, $p < 0.001$; ****, $p < 0.0001$.

An additional three females from each group were euthanized at 3 dpi to evaluate resident lung cells secreting IFN-γ, TNF-α, and IL-4. Data showed increased levels of IFN-γ and TNF-α, but no IL-4 in the vaccinated groups, consistent with the Th1-biased immune response elicited by the SAM vaccine in mice, and indicating a shift of the immune response away from a Th2 response that is associated with the risk of enhanced lung immunopathology (Figure S5C).

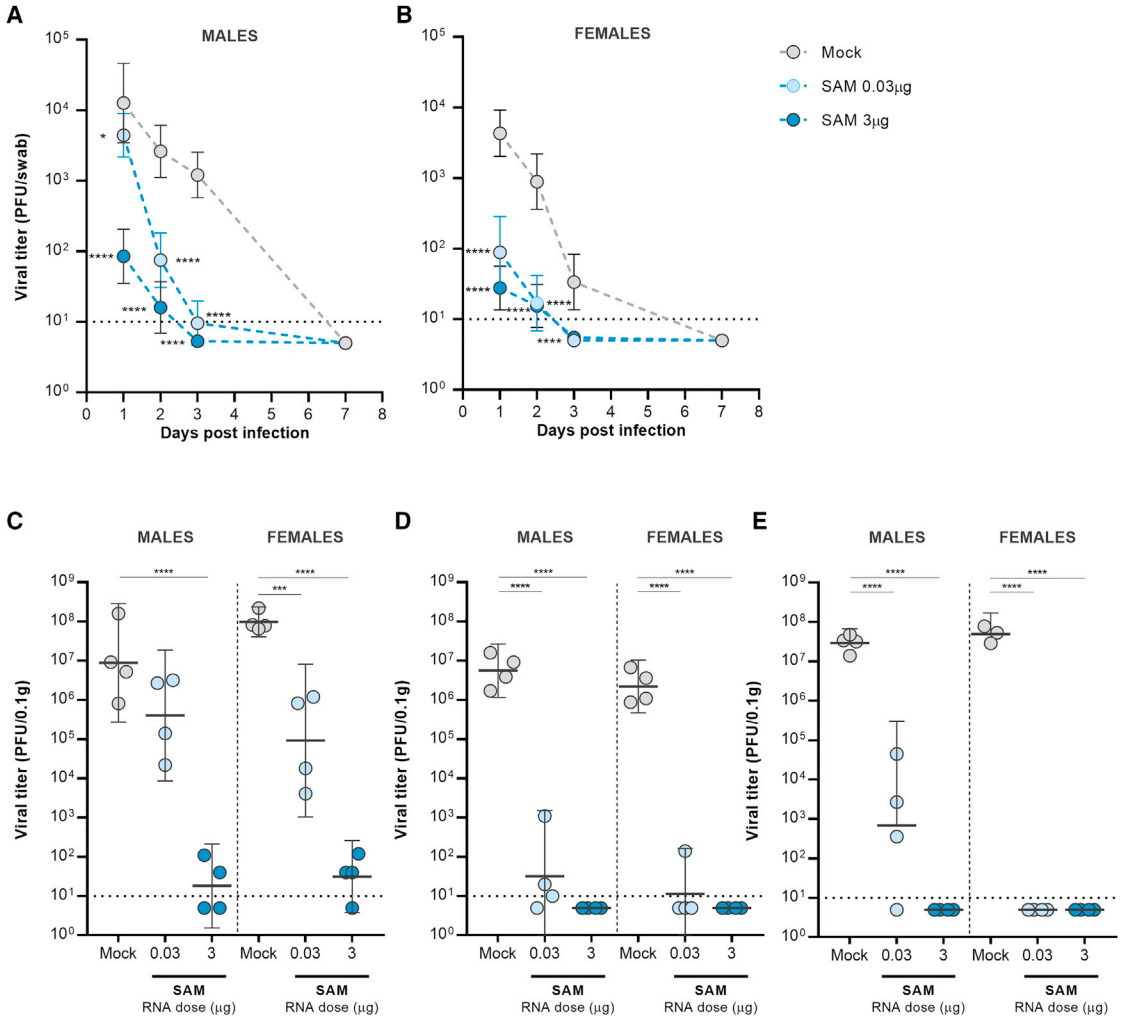

Figure 4. Viral loads from oropharyngeal swabs and respiratory tract tissues in SARS-CoV-2 SAM (LNP) vaccinated hamsters after challenge with SARS-CoV-2 virus

(A and B) Oropharyngeal swabs were taken from all hamsters on 1, 2, 3, and 7 dpi, and viral titers were determined by plaque assay. (C–E) Virus titers were determined in nasal turbinates (C), cranial right (D), and caudal right (E) lung lobes of four female and four male hamsters from each group at 3 dpi. Bars represent GMT+95% CI. Asterisks above bars indicate statistically significant difference in viral titers between mock and vaccine groups (****, $p < 0.0001$; ***, $p < 0.001$). Horizontal dotted line denotes limit of detection.

The remaining hamsters were observed until the study's endpoint at 21 dpi for body weight, body temperature, and clinical sign changes. Both the low- and high-dose SAM vaccinations prevented significant weight loss in both male and female hamsters compared with the mock vaccinated animals by 21 dpi ($p < 0.01$) (Figures S6A and S6B). The maximum percentage loss in body weight between the low-and high-dose SAM vaccinated groups was not statistically different (4.2% low-dose and 2.1% high-dose groups). Mock vaccinated hamsters lost an average maximum body weight of 11% by 21 dpi. No significant changes in body temperature, as measured by thermal microchips, were observed in any of the challenged groups (Figures S6C and S6D).

To further evaluate the efficacy of the SARS-CoV-2 SAM (LNP) vaccine candidate and any potential vaccine-mediated enhanced respiratory disease following challenge with SARS-CoV-2, hematoxylin and eosin (H&E) stained sections of the lungs (left lung and median lobe of the right lung; Figure 5), trachea, brain, liver, kidney, spleen, thymus, heart, and adrenal gland were microscopically evaluated at 3, 7, and 21 dpi. Naive non-infected hamsters (four females and four males) were euthanized at 21 dpi and included as a baseline control (Figure 5C). Histopathological examination of samples of the brain, liver, kidney, spleen, thymus, heart, and adrenal gland revealed no notable vaccine- or virus-related changes in SARS-CoV-2 SAM (LNP) vaccinated animals following virus challenge (data not shown). SARS-CoV-2 infection in mock vaccinated animals caused

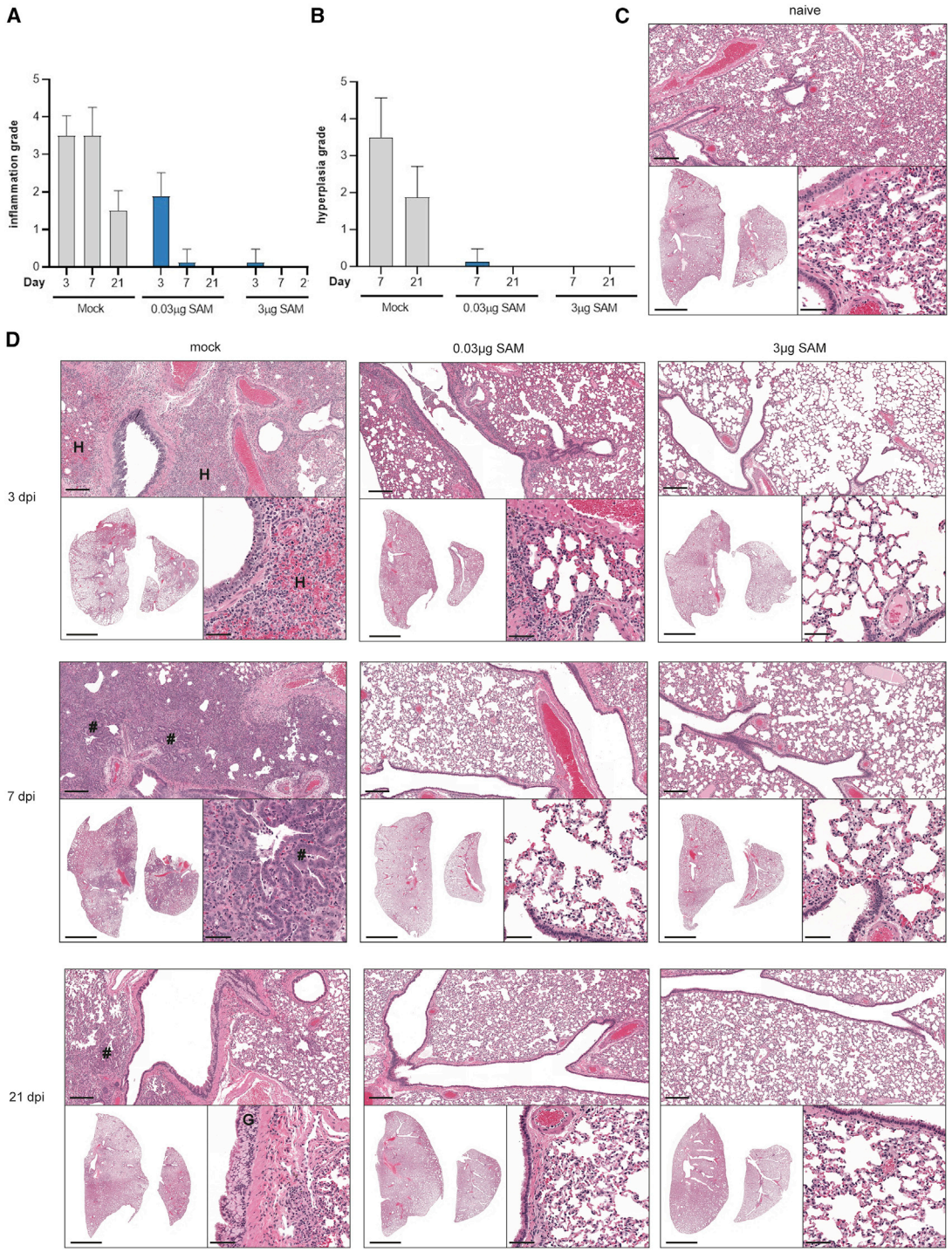

Figure 5. Histopathology following SARS-CoV-2 challenge of SARS-CoV-2 SAM (LNP) and mock vaccinated hamsters

(A) Lung pathology grading, with respect to inflammation (A) and centriacinar/bronchioloalveolar epithelial hyperplasia (B) in male and female hamsters necropsied at 3, 7, and 21 dpi with SARS-CoV-2 virus. (C) Representative lung sections from a naive male hamster showing the background level of atelectasis that can occur during necropsy. (D) Representative lung sections from mock vaccinated, SAM low dose (0.03µg), and SAM high dose (3µg) vaccinated male animals infected with SARS-CoV-2 virus and necropsied at 3, 7, and 21 dpi (histopathological features in females are consistent with those in males, females not shown). Sections are stained with H&E, and whole slide

(legend continued on next page)

the most severe pulmonary histopathology (Figures 5A–5D). At 3 dpi, histopathological features of SARS-CoV-2 infection in this group included moderate or severe inflammation predominantly surrounding large conducting airways and their associated large blood vessels and the terminal bronchioles and alveolar ducts. The inflammatory changes were characterized by a mixed cellular infiltrate composed predominantly of polymorphonuclear cells (PMNs) with fewer macrophages and lymphocytes throughout the affected areas of lung. PMNs were present within the airway epithelium and lumen and surrounding large blood vessels. The inflammatory infiltrate was associated with varying levels of necrosis of alveolar pneumocytes and/or capillary endothelia, hemorrhage, and edema. A dose-dependent reduction in the incidence and severity of inflammation was observed in vaccinated animals (Figure 5). Most of the 0.03 μg SARS-CoV-2 SAM (LNP) vaccinated animals had minimal or mild changes. Among the hamsters given the 3 μg dose, one male had minimal inflammation in the lung, whereas all females and the other three males exhibited normal lung morphology. By 7 dpi, mild to marked lung inflammation was observed in the mock vaccinated animals, similar to that observed at 3 dpi (Figure 5). A marked reduction in both the incidence and severity of the inflammatory and epithelial changes was observed in lungs of animals from both vaccine-treated groups when compared with the mock vaccinated animals. In the 0.03 μg dose group, minimal inflammation and epithelial hypertrophy/hyperplasia were observed in one male, with no changes noted in the other seven of eight animals in this treatment group. For the high dose group (3 μg), the lungs of all animals (eight of eight) were morphologically normal. By 21 dpi, inflammatory changes in the lung of the mock vaccinated animals had a similar distribution to that seen at 3 and 7 dpi, but were notably reduced in severity, with minimal or mild changes observed in all animals. Multifocal mild to marked hypertrophy/hyperplasia of the goblet cells of the bronchial epithelium was observed in all unvaccinated animals, reflecting an expected metaplastic response to chronic cell injury following SARS-CoV-2 viral infection. None of these findings were present in animals given either the 0.03 μg or 3 μg dose of the SAM vaccine candidate prior to SARS-CoV-2 exposure (Figure 5B).

In the trachea at day 3, minimal to moderate multifocal mixed inflammatory cell infiltrates were observed within the lamina propria in seven of eight mock vaccinated animals and were associated with focal hemorrhage in some instances. A similar level of inflammatory infiltrate was observed in the trachea from the SAM low-dose group animals, with all (eight of eight) animals having minimal or mild changes. In the SAM high-dose group, a reduction in incidence and severity of inflammatory infiltrates was observed (minimal severity, four of eight animals) and epithelial erosion, luminal exudate, or hemorrhage in the lamina propria were absent. At day 7, minimal or mild multifocal mixed inflammatory cell infiltrates, associated with minimal hemorrhage or occasional erosion, were observed in the trachea of some mock vaccinated animals (six of eight). A dose-associated reduction in incidence and severity of these changes was observed in vaccinated animals, with changes limited to minimal inflammatory cell infiltrates in three of eight animals from the SAM low-dose groups, while all SAM high-dose vaccinated animals had normal tracheal morphology. At day 21 there were no findings in the trachea of any animal exposed to SARS-CoV-2.

In summary, these data show that the SARS-CoV-2 SAM (LNP) vaccine candidate induced robust and protective adaptive immunity, which reduced virus load in the upper and lower airways of hamsters and protected them against weight loss and lung pathology following challenge with SARS-CoV-2. No evidence of enhanced respiratory disease was found in any of the vaccinated animals.

Repeated-dose toxicology and biodistribution of SARS-CoV-2 SAM (LNP) candidate vaccine in Sprague-Dawley rats

To further support the development of the SARS-CoV-2 SAM (LNP) vaccine, studies were conducted in Sprague-Dawley rats to assess the local tolerance, potential local and/or systemic toxicity, and biodistribution of the vaccine. The rat was selected for this purpose as this species is considered immunologically relevant and is a routine species for the toxicity testing of vaccines.[24,25] The rat also expresses toll-like receptor 7 (TLR7), among other TLRs and RNA sensors, which participate in the immune recognition of RNA.[7,26]

The repeated-dose toxicity study was conducted in male and female rats to characterize the vaccine's potential local and systemic toxicity after 3 i.m. injections (12 μg RNA/vaccination; saline was used as a mock control) at 2-week intervals and included a 4-week treatment-free period after the third vaccination (Figure S7A). Overall, the SARS-CoV-2 SAM (LNP) vaccine was well-tolerated. Induction of spike-specific IgG binding antibody responses was confirmed in 100% of the rats at day 32 and day 57 (i.e., 3 and 28 days following the third immunization) (Figure S8A). Injection site observations included very slight erythema after each immunization, persisting until 72 h post vaccination, and swelling (edema) following the second and/or third administration in some animals, which generally did not persist longer than 48 h post vaccination. The body weight of the animals was not affected by the consecutive administrations of the SAM vaccine candidate (Figure S8B).

Slight transient increases in mean rectal temperatures in SAM vaccinated animals were measured after each dose compared to the control group (i.e., mean changes up to ~2°C in males and females up to 48 h

images were obtained using P250 scanner (3D Histech). Representative low-power (bottom left, scale bar 5 mm), medium-power (top, scale bar 200 μm), and higher power (bottom right, scale bar 50 μm) photomicrographs are shown from each group. "#," hyperplasia of type II pneumocytes and bronchiolization of alveoli; "G," hyperplasia of goblet cells within bronchial epithelium; "H," areas of alveolar wall necrosis and hemorrhage within regions of inflammation. Further description of the histopathology at each time point is provided in the main text.

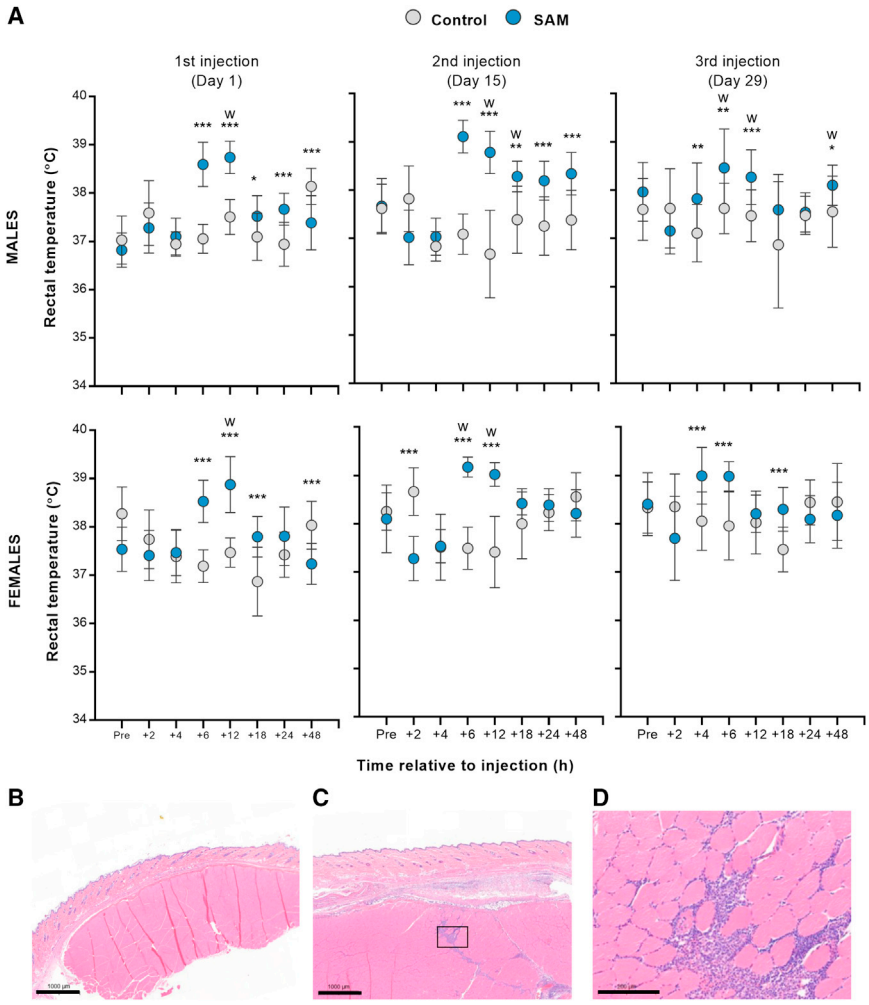

Figure 6. Repeated-dose toxicology assessment in SARS-CoV-2 SAM (LNP) vaccinated rats

(A) Body temperature. Male and female rats were immunized on three occasions (day 1, 15, and 29) with 12 μg of SARS-CoV-2 SAM (LNP) or saline. Rectal temperatures were measured 1 h before (Pre) and 2, 4, 6, 12, 18, 24, and 48 h post immunization. Results are shown as mean with SD. Statistical analysis: *, $p < 0.05$; **, $p < 0.01$; ***, $p < 0.001$ with t test, except those labeled "w," which was analyzed using Wilcoxon's test. The injection site sections, which include skin, dermis, and underlying skeletal muscle, from saline (B) or SAM (C) vaccinated animals at day 33 (3 days post third vaccination) were stained with H&E, and representative photomicrographs are represented (scale bar, 1,000 μm). (D) 5× magnification of the boxed area in (C) showing inflammation after SAM vaccination (scale bars, 200 μm).

following vaccination) (Figure 6A). There were no SARS-CoV-2 SAM (LNP)-related ophthalmological findings during this study.

At days 2 and 30, there were transient effects on hematology parameters relative to the control group, i.e., increased white blood cells (up to 1.40-fold) and neutrophils (up to 7.97-fold), and decreased lymphocyte (0.30-fold) and monocyte (0.67-fold) counts (Tables S1 and S2). Additionally, decreases in platelets (0.75-fold), coagulation (increased fibrinogen and partial thromboplastin times [PTT]), and clinical chemistry parameters were observed. These changes were considered related to the local inflammatory response and/or immune stimulation expected upon vaccination, and either improved or completely recovered by days 8, 36, and 57. Minimal transient increases of serum aspartate aminotransferase and alanine aminotransferase were noted in females on days 2 and 30, with no histopathological correlate (Tables S2 and S3).

Increased organ weights noted on day 32 in the iliac, inguinal, and popliteal lymph nodes were likely related to increased cellularity of the medullary cords (minimal to moderate), characterized by increased numbers of lymphocytes, plasma cells, and macrophages. This was considered secondary to the expected immune stimulation of the SAM vaccine candidate within the regional lymphoid tissue draining the injection site (Table S3). After the 4-week recovery period, there were no organ weight differences noted between groups.

Microscopic findings occurred primarily at the injection sites and draining lymph nodes. The SARS-CoV-2 SAM (LNP) vaccine candidate induced an increased incidence and severity of subcutaneous and muscular inflammation and/or hemorrhage at injection sites (Figures 6B and 6C). In the affected muscle, the predominant inflammation extended down fascial planes between muscle bundles or was within intermysial regions (Figure 6D). Nonetheless, these findings were considered a consequence of the expected immune response at the site of administration.

To evaluate the distribution of SARS-CoV-2 SAM (LNP) over time, a biodistribution study was performed (Figure S7B). Male and female rats received a single i.m. administration of 6 μg of the SAM vaccine candidate or saline as a mock control at day 1 and then distribution of RNA in tissues of vaccinated animals was analyzed at days 2, 8, 15, 29, and 60 by quantitative reverse transcription polymerase chain reaction (qRT-PCR) (Table 1).

At day 2, SAM RNA was detected with relatively high levels in muscle, lymph nodes, and spleen, and relatively lower levels in heart, liver, gonads, lungs, gonads, and blood. RNA levels progressively decreased in quantity in all tissues by day 60, but remained detectable in lymph nodes, spleen, and muscle, with at even lower quantities in the kidneys and livers of females. RNA was detectable in the testes only

Table 1. Biodistribution study

Tissues	Day 2	Day 8	Day 15	Day 29	Day 60
Injection site	Positive: 10 animals (3.5×10^7)	Positive: 9 animals (2.5×10^6)	Positive: 9 animals (2.5×10^3)	Positive: 5 animals (1.1×10^4)	Positive: 5 animals (5.3×10^2)
Popliteal lymph node	Positive: 10 animals (5.3×10^6)	Positive: 10 animals (4.9×10^5)	Positive: 10 animals (8.1×10^5)	Positive: 10 animals (5.7×10^5)	Positive: 10 animals (1.7×10^5)
Iliac lymph node	Positive: 10 animals (5.2×10^6)	Positive: 10 animals (3.0×10^6)	Positive: 10 animals (1.8×10^6)	Positive: 10 animals (1.5×10^6)	Positive: 10 animals (5.7×10^5)
Inguinal lymph node	Positive: 10 animals (6.5×10^5)	Positive: 10 animals (1.2×10^5)	Positive: 10 animals (1.7×10^4)	Positive: 10 animals (1.5×10^5)	Positive: 10 animals (8.0×10^4)
Spleen	Positive: 10 animals (5.4×10^5)	Positive: 10 animals (3.1×10^5)	Positive: 10 animals (1.3×10^5)	Positive: 10 animals (1.3×10^4)	Positive: 10 animals (2.1×10^3)
Heart	Positive: 10 animals (2.2×10^3)	Positive: 4 animals (4.2×10^2)	Positive: 4 animals (1.3×10^2)	Positive: 2 animals (2.5×10^2)	NP
Liver	Positive: 7 animals (5.6×10^3)	Positive: 5 animals (1.2×10^3)	Positive: 4 animals (5.1×10^2)	Positive: 1 animal (7.7×10^1)	Positive: 2 animals (4.1×10^2)
Kidney	Positive: 10 animals (7.2×10^2)	Positive: 8 animals (7.2×10^2)	Positive: 3 animals (1.7×10^2)	Positive: 1 animal (7.0×10^1)	Positive: 1 animal (7.7×10^1)
Ovaries	Positive: 5 animals (3.6×10^3)	Positive: 2 animals (8.4×10^1)	NP	NP	NA
Testis	Positive: 3 animals (2.0×10^2)	NP	NP	NA	NA
Lung	Positive: 10 animals (2.8×10^3)	Positive: 6 animals (4.8×10^2)	Positive: 5 animals (1.3×10^2)	NP	NP
Brain	NP	NP	NA	NA	NA
Blood	Positive: 10 animals (4.2×10^4)	Positive: 10 animals (2.7×10^2)	Positive: 3 animals (7.6×10^1)	NP	NP

Quantification of SAM RNA in blood and tissue samples after a single injection of 6 μg of SARS-CoV-2 SAM (LNP) at day 1. For all organs, n = 10, except for testes and ovaries (n = 5). NA, not analyzed; NP, no positive. Values in parentheses are mean values (mean copies/μg RNA).

on day 2 and in the ovaries on day 2 and day 8. Additionally, SARS-CoV-2 SAM was detected for longer periods in the liver of the females relative to the males. SAM RNA was not detected in any tissues at any time point in the saline control group, neither in the brain in any group at any time point.

Altogether, these results demonstrated that repeated administration of the SARS-CoV-2 SAM (LNP) vaccine candidate was well-tolerated and immunogenic in Sprague-Dawley rats. The biodistribution data demonstrated a prominent RNA signal in the muscle and draining lymph nodes up to 60 days following a single injection, with transient systemic dissemination at distal sites, with the exception of the brain.

DISCUSSION

A remarkable scientific effort since the onset of COVID-19 has led to the rapid development and approval of vaccines for emergency use, followed by full licensure of the first COVID-19 vaccine in August 2021.[3,4,27] However, multiple types and doses of vaccines will be needed to meet the demand of vaccinating the world's population and to tackle continuously emerging variants. Here, we describe a comprehensive preclinical assessment of a SARS-CoV-2 SAM (LNP) vaccine candidate, which uses the SAM technology expressing the prefusion-stabilized full-length spike antigen that was delivered by an LNP formulation. We have demonstrated that the SARS-CoV-2 SAM (LNP) vaccine induces strong antigen-specific immune responses in mice, has a favorable safety profile in rats, and protects hamsters against a SARS-CoV-2 virus challenge.

In mice, after the first and second immunization with sub-microgram doses of the SARS-CoV-2 SAM (LNP) candidate vaccine, robust neutralizing antibody titers were observed, which were similar to and greater than the titers of a panel of SARS-CoV-2-convalescent human sera, respectively. The magnitude, longevity, and quality of antibody responses induced by a vaccine is determined by its ability to induce GC reactions that lead to differentiation of memory B cells and long-lived plasma cells.[21] We found that the SARS-CoV-2 SAM (LNP) vaccine elicited robust spike-specific class-switched B cells and GC responses, suggesting a potential induction of high-affinity long-lasting B cells, which are critical for long-term protection and recovery from SARS-CoV-2 infection.[28] Testing at later time points after a single- or a two-immunization regimen could help determine the longevity of this response and the effectiveness of a possible single-dose regimen.

A SARS-CoV-2 vaccine should be effective against the emergence of SARS-CoV-2 variants of concern with either increased transmission or virulence. In mice, our vaccine candidate elicited significant

neutralizing antibody titers against SARS-CoV-2 B.1.1.7, B.1.351, and B.1.617.2 variants, although with a reduction in titers compared to the Wuhan virus, consistent with the reports for other mRNA vaccines.[29] These data suggest the potential use of this SAM vaccine to boost pre-existing SARS-CoV-2 immunity obtained either by natural infection or vaccination to protect against emerging virus variants. Additionally, thanks to its manufacturing flexibility, this vaccine technology, in combination with antigen design, might be employed to quickly develop variant-matched vaccines to tackle continuously emerging SARS-CoV-2 variants of concern.

In mice, our SAM vaccine candidate induced potent Th1-biased $CD4^+$ T cell responses, which are desirable for an effective and safe SARS-CoV-2 vaccine. The vaccine also induced high levels of spike-specific polyfunctional cytotoxic $CD8^+$ T cells, which could contribute to viral clearance upon infection, as suggested by previous reports on mouse infection models of SARS-CoV and MERS-CoV, and more importantly, by recent reports on better recovery from COVID-19.[30,31]

One essential step during vaccine development is the evaluation of efficacy and safety of the candidate vaccine. SARS-CoV-2 vaccines based on a self-amplifying RNA platform have been previously shown to be immunogenic in NHPs and efficacious in hACE2 transgenic mice.[10,32,33] However, no information is available on the protective efficacy of self-amplifying mRNA vaccines in an animal model manifesting some of the hallmarks of severe COVID-19 disease. The hamster study presented here is the first study to our knowledge to test a self-amplifying mRNA SARS-CoV-2 vaccine candidate in such animal challenge model. Following exposure to live SARS-CoV-2 virus, non-vaccinated hamsters produce and shed virus for several days post exposure, develop clinical signs, lose weight, and develop severe pneumonia similar to COVID-19 patients, and therefore are an important model for preclinical vaccine efficacy studies.[22,23] In the present study, a single SARS-CoV-2 SAM (LNP) vaccination induced neutralizing antibody titers in hamsters, which were further boosted by a second vaccination. Two administrations of the SARS-CoV-2 SAM (LNP) vaccine protected hamsters against SARS-CoV-2 virus challenge, clearing virus load in the upper and lower airways, and preventing weight loss, lung pathology, and severe disease. Even at the 0.03 μg RNA dose, the protection of the SAM vaccines against SARS-CoV-2 lung pathology was readily apparent. This is in contrast to the optimized conventional SARS-CoV-2 mRNA vaccines, which have been previously shown to provide protection against lung injury and weight loss in SARS-CoV-2 infected hamsters with a two-dose regimen at the 5 μg dose.[34] SAM (LNP) vaccine drastically reduced lung disease in the same model at extremely low RNA doses (0.03 μg), highlighting the dose-sparing potential of the SAM vaccine technology,[10] which will be also reflected in the lower vaccine doses to be tested in clinical setting. To address pandemics, such as COVID-19, where several billion doses of vaccines are needed within months, a lower vaccine dose required for protection, i.e., dose sparing, would be extremely beneficial. Interestingly, in this hamster study, female and male animals responded differently to the SARS-CoV-2 SAM (LNP) vaccine, and the female animals had higher neutralizing antibody titers and lower viral titers at the low vaccine dose (0.03 μg RNA). As noted in several studies (for reviews, see Klein and Flanagan [35] and Fischinger et al.[36]), females typically develop more robust antibody responses following vaccination than their male counterparts. Dissection of the mechanisms that underlie gender differences in vaccine-induced immunity is complex and has implicated hormonal, genetic, and environmental differences between females and males, and the deep analyses required to study these elements exceed the scope of the studies reported herein. Importantly, no evidence of enhanced respiratory disease was found in any of the vaccinated hamsters, which is consistent with the Th1 cytokine signature produced by resident lung cells seen in the vaccinated animals as well as the Th1 CD4+ T cell response observed in mice.

Given the novelty and the early stage of the SAM technology, we evaluated its potential toxic effects and biodistribution in rats. After two administrations, the clinical signs were limited to slight local irritation at the injection site (erythema and/or edema), which did not persist for more than 48 h post vaccination. After each vaccination, there was also transient increase at 6- and 12-h post administration in mean rectal temperatures. This might be indicative of innate immune responses triggered by the RNA and lipid formulation used for delivery and/or process-derived dsRNA and short aborted mRNA not completely removed from the vaccine.[37,38] Self-amplifying mRNA molecules are at least 10 kb in length and present additional challenges for purification compared with conventional mRNA molecules. Preliminary data in mice have shown that the intracellular influx of the self-amplifying mRNA, rather than its amplification, is mainly responsible for eliciting type I IFN response.[39] However, additional studies are needed to dissect the contribution of incoming and amplifying mRNA to innate activation and possible vaccine reactogenicity. Inflammatory responses, indicating the establishment of an innate immune response, were also observed with transient and reversible effects on hematology and chemistry parameters and by the activated appearance of the draining lymph nodes, at both the microscopic and macroscopic levels. Overall, these changes were similar to those seen after the administration of a cationic nanoemulsion (CNE) formulated SAM vaccine as well as of conventional vaccines, including adjuvanted recombinant proteins and virus-like particles-based vaccines.[40–42]

In the biodistribution study in rats, the vaccine-delivered RNA was found in the muscle at the injection site until 60 days post vaccination. RNA was also found in the draining lymph nodes at day 2, suggesting that it quickly traffics to the host's lymphoid organs. It remains unclear, however, whether the RNA distributed to the lymph nodes or whether it entered immune cells that subsequently trafficked to the lymph nodes. Similar to the previous report on a CNE-formulated SAM vaccine,[40] SAM RNA was detected also at systemic sites, including spleen, blood, lung, and liver. Although expression from

an LNP-delivered self-amplifying mRNA has been reported in the draining lymph nodes of mice after intradermal administration,[43] it remains to be determined whether the signal found in the various organs for a prolonged period of time in our study is from injected material or amplified material (i.e., generation of multiple RNA copies through self-amplification in target cells), and whether it represents full-length RNA or truncated pieces of RNA resulting from degradation.

Our study describes the full preclinical development of a SARS-CoV-2 SAM (LNP) vaccine and supports its current evaluation in a first-in-human phase 1 clinical trial (NCT04758962). Other vaccine candidates based on synthetically delivered self-amplifying mRNA are in earlier stages of clinical testing. Preliminary data from a phase I clinical trial (ISRCTN Register: ISRCTN17072692) show tolerability up to 10 μg RNA dose of an LNP-formulated self-amplifying mRNA-based SARS-CoV-2 vaccine, although immunogenicity based on spike-specific antibodies was inferior (65% seroconversion) to the currently approved COVID-19 mRNA vaccines, despite promising responses previously observed with the same candidate in mice.[33,44] The reasons for the low humoral responses in humans have not been identified, and it will be critical to generate clinical data from other SAM-based vaccines to fully understand the potential of this technology. Each SAM vaccine candidate could have different performance in humans, for example, due to difference in RNA sequences and manufacturing processes, levels of purity, enrichment in full-length SAM molecules, and delivery systems.

The results from the ongoing GSK clinical trial will inform if the current SAM vaccine is sufficiently tolerated and immunogenic, or if further optimization, including RNA engineering, new delivery systems, and modulation of innate and adaptive immune responses, among others, will be needed, contributing to define the true prospects of the technology.

MATERIALS AND METHODS

Study design

The primary objective of these studies was to determine and characterize the immunogenicity, protective efficacy, safety, and biodistribution of a SARS-CoV-2 SAM (LNP) vaccine candidate in preclinical models (mice, hamsters, and rats). Group sizes were based on previous experiments using a similar SAM platform. Endpoints were selected before the start of each study based on primary and secondary objectives of each study. Replication of experiments, number of biological and technical replicates, and randomization varied among experiments as described subsequently and in figure legends. Ethical and non-clinical guidelines are described in the supplemental information.

SARS-CoV-2 SAM vaccine preparation

The antigen sequences of SARS-CoV-2 full-length spike were based on the Wuhan-Hu-1 strain of SARS-CoV-2 virus (GenBank: MN908947), a codon optimized for expression in mammalian cells ($spike_{FL}$), and mutagenized with prefusion-stabilizing proline substitutions (antigen amino acid residues 986 and 987) together with a "GSAS" substitution at the furin cleavage site (antigen residues 682–685)[16] ($spike_{FL\text{-}2P}$). The spike antigens were cloned in DNA plasmids encoding the SAM backbone using standard molecular techniques. *In vitro* RNA transcription, purification, and LNP formulation were performed as described previously[6,45,46] and in the supplemental information. *In vitro* characterization of the SARS-CoV-2 SAM (LNP) vaccine is described in the supplemental information.

Mouse immunogenicity studies

The mouse studies were carried out at GSK (Upper Providence, PA). Female BALB/c mice 7–8 weeks of age (Charles River, Raleigh, NC) (n = 10 mice/group; randomly distributed between groups) received 2 i.m. injections 3 weeks apart in the hind leg thigh muscle with the SARS-CoV-2 SAM (LNP) vaccine at three dose levels of 1.5 μg, 0.15 μg, or 0.015 μg RNA or saline (mock). Serum samples were collected 21 days after the first immunization (3wp1) and 14 days after the second immunization (2wp2) to assess IgG binding and neutralizing antibody titers, as described in the supplemental information. Spleens and draining inguinal lymph nodes were collected 2wp2 to characterize spike-specific B cell and $CD4^+$ and $CD8^+$ T cell responses, as described in the supplemental information. Details of the mice study design are provided in Figure S2A.

Hamster immunogenicity and challenge study

The hamster study was carried out at Colorado State University (Fort Collins, CO). Male and female Golden Syrian hamsters (*Mesocricetus auratus*) approximately 8 weeks of age (Envigo, Indianapolis, IN) (n = 27 animals/group, 15 females and 12 males) received 2 i.m. injections, 3 weeks apart in the hind leg thigh muscle with the SARS-CoV-2 SAM (LNP) vaccine at a dose of 3 μg or 0.03 μg or with saline (mock). A non-treated group of hamsters (n = 8, four females and four males) was also included in the study to provide a baseline for the histopathologic analysis. Serum samples were collected 21 days after the first immunization (3wp1) and 21 days after the second immunization (3wp2) to assess neutralizing antibody titers. Three weeks after the second immunization, hamsters were anesthetized (ketamine-xylazine) and challenged under BSL3 containment by intranasal instillation of 10^4 PFU of the USA-WA1/2020 isolate of SARS-CoV-2 virus (product NR-52281, BEI resources) propagated in Vero C1008 cells (Vero E6) as previously described.[47]

Animals were monitored for body weights and temperatures (thermal microchips) once daily starting at one day prior to viral challenge and continuing until the day of scheduled euthanasia. Oropharyngeal swabbing for viral load assessment in the upper respiratory tract was performed on days 1, 2, 3, and 7 post challenge. Samples were collected in viral transport medium, frozen at −80°C, and assayed for virus by plaque assay on Vero cells.

Scheduled euthanasia of eight hamsters per group (four males and four females) was performed on days 3 (acute), 7 (subacute), and 21 (resolving) post challenge. At day 3, nasal turbinates and two lobes

of lung (cranial and caudal lobes of the right lung) were harvested for virus titration by plaque assay on Vero cells. At days 3, 7, and 21, a selected panel of tissues was harvested for macroscopic observation and histopathology. Details of the hamster study design are provided in Figure S5A, while methods for plaque assay, cytokine profiling, and histopathology are described in the supplemental information.

Repeated-dose toxicity and biodistribution studies in Sprague-Dawley rats

Animals and descriptions of the study

Male and female Sprague-Dawley rats (*Rattus norvegicus*) were obtained from Charles River Laboratories (Laval, QC, Canada) and were acclimated for at least 12 days to be 10 weeks old at the initiation of dosing (day 1). The male rats weighed 310–388 g and the female rats weighed 205–271 g on day 1. The repeated-dose toxicity and biodistribution studies were carried out at the Charles River Laboratories (Laval, QC, Canada). Description of welfare principles and non-clinical guidelines[48,49] are described in the supplemental information.

Repeated-dose toxicity study

The dosing schedule (3 doses) was intended to cover the number of injections planned in human clinical trial subjects +1 additional dose (i.e., n + 1 dosing). During the acclimation period, 15 male and 15 female rats were allocated to two groups by a randomizing stratification system based on body weights. On days 1, 15, and 29, the animals received one i.m. injection of the SARS-CoV-2 SAM (LNP) vaccine (100 μL, corresponding to 12 μg RNA) into the posterior part of the thigh muscle. Animals in the control group received saline in the same conditions as in the treated groups. The study design is depicted in Figure S7A. Detailed methods for clinical examinations, serology, hematology, coagulation, and blood biochemistry investigations as well as for necropsy, tissue processing, and histopathological examination are provided in the supplemental information.

Biodistribution study

To evaluate the biodistribution of the SARS-CoV-2 SAM (LNP) vaccine, one i.m. injection (100 μL, corresponding to 6 μg RNA) was performed into the posterior part of the thigh muscle of the right hindlimb of male and female Sprague-Dawley rats. The biodistribution was evaluated in tissues by qRT-PCR on extracted RNA, targeting the non-structural region of the SAM construct, over a 59-day observation period (Figure S7B). Rats in the treatment group were randomly allocated into five subgroups (one group/time point) of 10 animals (five animals/sex/group). Treated animals were necropsied at days 2, 8, 15, 29, and 60. In the control group, five males and five females received an injection of saline, and one animal/sex was sacrificed at the same time points as in the treated groups.

At their respective scheduled termination (days 2, 8, 15, 29, and 60), animals were anesthetized with isoflurane and blood and tissues (brain, lung liver, spleen, kidneys, heart, gonads, lymph nodes [popliteal, inguinal, and iliac] and muscle at the injection site) were collected, preserved, and RNA was extracted and analyzed by qRT-PCR as previously described.[40] Detailed methods are described in the supplemental information.

Statistical analyses

Mixed model repeated measurements with group, day, and interaction between group and day as fixed effects with appropriate variance and co-variance structure were fitted on log10 transformed for spike-specific IgG binding antibody titers, $pVNT_{50}$ and VNT_{50} for the mouse data, and for $pVNT_{50}$ and oropharyngeal swab viral titers for each sex for the hamster data. An analysis of variance (ANOVA) was fitted on log10 transformed data with group as fixed factors with appropriate variance assumption for $pVNT_{50}$ and VNT_{50}, antigen-specific B cell and T cell responses in mice, and for nasal and lung tissue virus titer (nasal turbinates, cranial lung, caudal lung for each sex) in hamsters. For hamsters' body weight and body temperature, an ANOVA was performed with group as fixed factors on separated day for each sex. All data shown were derived from one experiment, except for B cells data where data from two individual experiments were combined. For the comparison of mean body weight, organ weights and relative organ weights, mean body temperature, food consumption, hematology, coagulation, clinical chemistry mean values or Draize-based scoring parameters in the rat study, statistical methods, and criteria were used following those described in Stokes et al.[40]

SUPPLEMENTAL INFORMATION

Supplemental information can be found online at https://doi.org/10.1016/j.ymthe.2022.01.001.

ACKNOWLEDGMENTS

We thank Shanshan Xu for *in vitro* testing of the LNP-formulated SAM vaccines; Jason Laliberte, Marco Biancucci, Sai Tian, Karen Matsuoka, and Ying Huang for cloning, expression, and purification of the recombinant SARS-CoV-2 spike protein used in the Luminex-based IgG binding antibody assay; Enrico Malito and Matthew J. Bottomley for antigen design advice; Leonard Azzarano for supporting the mouse studies; Ellen Gugel, Stephanie Fresnay, Maureen Stefaniak, and Glomil Corbin for supporting the mouse immunoassays; Jungeun Park for flow cytometry support; Bart Corsaro for human sample management; Madison Wallace for operational support; Erik Stemmy and Chelsea Lane from NIAID for coordinating the hamster study at Colorado State University through the National Institute of Allergy and Infectious Diseases (NIAID) preclinical study network.

This work was funded by GlaxoSmithKline Biologicals SA. The Shi laboratory has received funding support in sponsored research agreements from GSK, Pfizer, Gilead, IGM Biosciences, and Atea Pharmaceuticals. The hamster study was funded by the National Institute of Allergy and Infectious Diseases preclinical study network.

AUTHOR CONTRIBUTIONS

G.M., J.B.U., A.M.S., and D.Y. conceived and conceptualized the work and strategy. G.M., K.L., and J.W. designed constructs and planned *in vitro* studies; J.W. designed primers, performed oligo synthesis,

and cloned constructs. J.M. performed RNA synthesis and analysis; J.W. and L.Q. performed and analyzed *in vitro* studies. I.M. and R.Jo. managed the formulation of RNA. C.P.M, G.L., and G.M. designed mouse immunogenicity studies and analyzed and interpreted data. D.M. performed the mouse studies. G.L. and K.A. supported the mouse studies. K.F. and C.P.M. designed, performed, and analyzed the spike-binding IgG assays in mice and rat sera. J.Z. and X.X. performed the VNTs experiment. J.Z., X.X., and P.Y.S. interpreted the VNTs results. T.C., G.L., J.T.S., A.K., S.N., R.J., and S.B. planned, performed, and analyzed T and B cell responses in mice. A.H.S. designed rat toxicity and biodistribution studies, oversaw the studies, and analyzed and interpreted data. M.A.A. and C.S. performed and analyzed the rat toxicity and biodistribution studies and their readouts. M.J.G. and M.A.R. read and interpreted histopathology slides and data for the rat study. A.H.S., A.M.S., G.M., R.A.B., R.T., and C.P.M. designed the hamster study; A.H.S., R.A.B., and C.P.M. oversaw the hamster study, analyzed and interpreted data. T.D., I.R., M.H-T., and R.A.B. performed the hamster study, immunology and virology readouts, and analyzed the data. R.T. and A.R. read and interpreted histopathology slides and data from the hamster study. K-F.W. performed statistical analysis of readouts from the mice and hamster studies. G.M. and C.P.M. contributed to synthesis and integrated interpretation of obtained data. G.M. and C.P.M. wrote the manuscript. All authors supported the review of the manuscript.

DECLARATION OF INTERESTS

G.M., C.P.M., J.W., T.C., G.L., K.F., L.Q., J.T.S., J.M., A.K., K.A., K-F.W., I.M., R.T., A.R., M.A.R., A-M.S., R.Jo., S.N., R.J., K.L., S.B., J.B.U., A.H.S., and D.Y. are current or former employees of the GSK group of companies and may own GSK shares and/or restricted GSK shares. G.M., J.W., L.Q., K.L., J.B.U., and D.Y. are inventors on a patent application claiming subject matter related to the SARS-CoV-2 SAM vaccine candidates described herein. P.Y.S. is a member of the Scientific Advisory Boards of AbImmune and is Founder of Flavi-Tech. X.X. and P.-Y.S. have filed a patent on the reverse genetic system of SARS-CoV-2. M.A.A., M.G., and C.S. received compensation from GSK to perform the rat toxicity and biodistribution assays. The other authors declare no other competing interests.

REFERENCES

1. Sempowski, G.D., Saunders, K.O., Acharya, P., Wiehe, K.J., and Haynes, B.F. (2020). Pandemic preparedness: developing vaccines and therapeutic antibodies for COVID-19. Cell *181*, 1458–1463. https://doi.org/10.1016/j.cell.2020.05.041.
2. WHO (2021). Draft landscape and tracker of COVID-19 candidate vaccines. https://www.who.int/publications/m/item/draft-landscape-of-covid-19-candidate-vaccines.
3. Polack, F.P., Thomas, S.J., Kitchin, N., Absalon, J., Gurtman, A., Lockhart, S., Perez, J.L., Perez Marc, G., Moreira, E.D., Zerbini, C., et al. (2020). Safety and efficacy of the BNT162b2 mRNA covid-19 vaccine. N. Engl. J. Med. *383*, 2603–2615. https://doi.org/10.1056/NEJMoa2034577.
4. FDA (2021). FDA approves first COVID-19 vaccine. https://www.fda.gov/news-events/press-announcements/fda-approves-first-covid-19-vaccine.
5. Hekele, A., Bertholet, S., Archer, J., Gibson, D.G., Palladino, G., Brito, L.A., Otten, G.R., Brazzoli, M., Buccato, S., Bonci, A., et al. (2013). Rapidly produced SAM((R)) vaccine against H7N9 influenza is immunogenic in mice. Emerg. Microbes Infect. *2*, e52. https://doi.org/10.1038/emi.2013.54.
6. Geall, A.J., Verma, A., Otten, G.R., Shaw, C.A., Hekele, A., Banerjee, K., Cu, Y., Beard, C.W., Brito, L.A., Krucker, T., et al. (2012). Nonviral delivery of self-amplifying RNA vaccines. Proc. Natl. Acad. Sci. U S A *109*, 14604–14609. https://doi.org/10.1073/pnas.1209367109.
7. Pepini, T., Pulichino, A.M., Carsillo, T., Carlson, A.L., Sari-Sarraf, F., Ramsauer, K., Debasitis, J.C., Maruggi, G., Otten, G.R., Geall, A.J., et al. (2017). Induction of an IFN-mediated antiviral response by a self-amplifying RNA vaccine: implications for vaccine design. J. Immunol. *198*, 4012–4024. https://doi.org/10.4049/jimmunol.1601877.
8. Vogel, A.B., Lambert, L., Kinnear, E., Busse, D., Erbar, S., Reuter, K.C., Wicke, L., Perkovic, M., Beissert, T., Haas, H., et al. (2018). Self-amplifying RNA vaccines give equivalent protection against influenza to mRNA vaccines but at much lower doses. Mol. Ther. *26*, 446–455. https://doi.org/10.1016/j.ymthe.2017.11.017.
9. Erasmus, J.H., Khandhar, A.P., Guderian, J., Granger, B., Archer, J., Archer, M., Gage, E., Fuerte-Stone, J., Larson, E., Lin, S., et al. (2018). A nanostructured lipid carrier for delivery of a replicating viral RNA provides single, low-dose protection against zika. Mol. Ther. https://doi.org/10.1016/j.ymthe.2018.07.010.
10. de Alwis, R., Gan, E.S., Chen, S., Leong, Y.S., Tan, H.C., Zhang, S.L., Yau, C., Low, J.G.H., Kalimuddin, S., Matsuda, D., et al. (2021). A single dose of self-transcribing and replicating RNA-based SARS-CoV-2 vaccine produces protective adaptive immunity in mice. Mol. Ther. *29*, 1970–1983. https://doi.org/10.1016/j.ymthe.2021.04.001.
11. Sanders, N.N. (2021). Low-dose single-shot COVID-19 mRNA vaccines lie ahead. Mol. Ther. *29*, 1944–1945. https://doi.org/10.1016/j.ymthe.2021.05.003.
12. Wu, F., Zhao, S., Yu, B., Chen, Y.M., Wang, W., Song, Z.G., Hu, Y., Tao, Z.W., Tian, J.H., Pei, Y.Y., et al. (2020). A new coronavirus associated with human respiratory disease in China. Nature *579*, 265–269. https://doi.org/10.1038/s41586-020-2008-3.
13. Yi, C., Sun, X., Ye, J., Ding, L., Liu, M., Yang, Z., Lu, X., Zhang, Y., Ma, L., Gu, W., et al. (2020). Key residues of the receptor binding motif in the spike protein of SARS-CoV-2 that interact with ACE2 and neutralizing antibodies. Cell. Mol. Immunol. *17*, 621–630. https://doi.org/10.1038/s41423-020-0458-z.
14. Yan, R., Zhang, Y., Li, Y., Xia, L., Guo, Y., and Zhou, Q. (2020). Structural basis for the recognition of SARS-CoV-2 by full-length human ACE2. Science *367*, 1444–1448. https://doi.org/10.1126/science.abb2762.
15. Jackson, C.B., Farzan, M., Chen, B., and Choe, H. (2021). Mechanisms of SARS-CoV-2 entry into cells. Nat. Rev. Mol. Cell Biol. https://doi.org/10.1038/s41580-021-00418-x.
16. Wrapp, D., Wang, N., Corbett, K.S., Goldsmith, J.A., Hsieh, C.L., Abiona, O., Graham, B.S., and McLellan, J.S. (2020). Cryo-EM structure of the 2019-nCoV spike in the prefusion conformation. Science *367*, 1260–1263. https://doi.org/10.1126/science.abb2507.
17. Tseng, C.T., Sbrana, E., Iwata-Yoshikawa, N., Newman, P.C., Garron, T., Atmar, R.L., Peters, C.J., and Couch, R.B. (2012). Immunization with SARS coronavirus vaccines leads to pulmonary immunopathology on challenge with the SARS virus. PLoS One *7*, e35421. https://doi.org/10.1371/journal.pone.0035421.
18. Bolles, M., Deming, D., Long, K., Agnihothram, S., Whitmore, A., Ferris, M., Funkhouser, W., Gralinski, L., Totura, A., Heise, M., and Baric, R.S. (2011). A double-inactivated severe acute respiratory syndrome coronavirus vaccine provides incomplete protection in mice and induces increased eosinophilic proinflammatory pulmonary response upon challenge. J. Virol. *85*, 12201–12215. https://doi.org/10.1128/JVI.06048-11.
19. Muruato, A.E., Fontes-Garfias, C.R., Ren, P., Garcia-Blanco, M.A., Menachery, V.D., Xie, X., and Shi, P.Y. (2020). A high-throughput neutralizing antibody assay for COVID-19 diagnosis and vaccine evaluation. Nat. Commun. *11*, 4059. https://doi.org/10.1038/s41467-020-17892-0.
20. Jhun, H., Park, H.Y., Hisham, Y., Song, C.S., and Kim, S. (2021). SARS-CoV-2 Delta (B.1.617.2) variant: a unique T478K mutation in receptor binding motif (RBM) of spike gene. Immune Netw. *21*, e32. https://doi.org/10.4110/in.2021.21.e32.
21. Sallusto, F., Lanzavecchia, A., Araki, K., and Ahmed, R. (2010). From vaccines to memory and back. Immunity *33*, 451–463. https://doi.org/10.1016/j.immuni.2010.10.008.
22. Imai, M., Iwatsuki-Horimoto, K., Hatta, M., Loeber, S., Halfmann, P.J., Nakajima, N., Watanabe, T., Ujie, M., Takahashi, K., Ito, M., et al. (2020). Syrian hamsters as a small

animal model for SARS-CoV-2 infection and countermeasure development. Proc. Natl. Acad. Sci. U S A *117*, 16587–16595. https://doi.org/10.1073/pnas.2009799117.

23. Chan, J.F., Zhang, A.J., Yuan, S., Poon, V.K., Chan, C.C., Lee, A.C., Chan, W.M., Fan, Z., Tsoi, H.W., Wen, L., et al. (2020). Simulation of the clinical and pathological manifestations of coronavirus disease 2019 (COVID-19) in a golden Syrian hamster model: implications for disease pathogenesis and transmissibility. Clin. Infect. Dis. *71*, 2428–2446. https://doi.org/10.1093/cid/ciaa325.

24. EMA-CPMP (1997). Note for guidance on preclinical pharmacological and toxicological testing of vaccines (CPMP/SWP/465/95). http://www.ema.europa.eu/docs/en_GB/document_library/Scientific_guideline/2009/10/WC500004004.pdf.

25. WHO (2003). WHO guidelines on nonclinical evaluation of vaccines. http://www.who.int/biologicals/publications/nonclinical_evaluation_vaccines_nov_2003.pdf.

26. Astakhova, N.M., Perelygin, A.A., Zharkikh, A.A., Lear, T.L., Coleman, S.J., MacLeod, J.N., and Brinton, M.A. (2009). Characterization of equine and other vertebrate TLR3, TLR7, and TLR8 genes. Immunogenetics *61*, 529–539. https://doi.org/10.1007/s00251-009-0381-z.

27. Baden, L.R., El Sahly, H.M., Essink, B., Kotloff, K., Frey, S., Novak, R., Diemert, D., Spector, S.A., Rouphael, N., Creech, C.B., et al. (2020). Efficacy and safety of the mRNA-1273 SARS-CoV-2 vaccine. N. Engl. J. Med. https://doi.org/10.1056/NEJMoa2035389.

28. Turner, J.S., O'Halloran, J.A., Kalaidina, E., Kim, W., Schmitz, A.J., Zhou, J.Q., Lei, T., Thapa, M., Chen, R.E., Case, J.B., et al. (2021). SARS-CoV-2 mRNA vaccines induce persistent human germinal centre responses. Nature *596*, 109–113. https://doi.org/10.1038/s41586-021-03738-2.

29. Wu, K., Werner, A.P., Moliva, J.I., Koch, M., Choi, A., Stewart-Jones, G.B.E., Bennett, H., Boyoglu-Barnum, S., Shi, W., Graham, B.S., et al. (2021). mRNA-1273 vaccine induces neutralizing antibodies against spike mutants from global SARS-CoV-2 variants. bioRxiv. https://doi.org/10.1101/2021.01.25.427948.

30. Channappanavar, R., Fett, C., Zhao, J., Meyerholz, D.K., Perlman, S., and Sandri-Goldin, R.M. (2014). Virus-specific memory CD8 T cells provide substantial protection from lethal severe acute respiratory syndrome coronavirus infection. J. Virol. *88*, 11034–11044. https://doi.org/10.1128/JVI.01505-14.

31. Grifoni, A., Weiskopf, D., Ramirez, S.I., Mateus, J., Dan, J.M., Moderbacher, C.R., Rawlings, S.A., Sutherland, A., Premkumar, L., Jadi, R.S., et al. (2020). Targets of T cell responses to SARS-CoV-2 coronavirus in humans with COVID-19 disease and unexposed individuals. Cell *181*, 1489–1501 e1415. https://doi.org/10.1016/j.cell.2020.05.015.

32. Erasmus, J.H., Khandhar, A.P., O'Connor, M.A., Walls, A.C., Hemann, E.A., Murapa, P., Archer, J., Leventhal, S., Fuller, J.T., Lewis, T.B., et al. (2020). An Alphavirus-derived replicon RNA vaccine induces SARS-CoV-2 neutralizing antibody and T cell responses in mice and nonhuman primates. Sci. Transl. Med. *12*. https://doi.org/10.1126/scitranslmed.abc9396.

33. McKay, P.F., Hu, K., Blakney, A.K., Samnuan, K., Brown, J.C., Penn, R., Zhou, J., Bouton, C.R., Rogers, P., Polra, K., et al. (2020). Self-amplifying RNA SARS-CoV-2 lipid nanoparticle vaccine candidate induces high neutralizing antibody titers in mice. Nat. Commun. *11*, 3523. https://doi.org/10.1038/s41467-020-17409-9.

34. Meyer, M., Wang, Y., Edwards, D., Smith, G.R., Rubenstein, A.B., Ramanathan, P., Mire, C.E., Pietzsch, C., Chen, X., Ge, Y., et al. (2021). Attenuated activation of pulmonary immune cells in mRNA-1273-vaccinated hamsters after SARS-CoV-2 infection. J. Clin. Invest. *131*. https://doi.org/10.1172/JCI148036.

35. Klein, S.L., and Flanagan, K.L. (2016). Sex differences in immune responses. Nat. Rev. Immunol. *16*, 626–638. https://doi.org/10.1038/nri.2016.90.

36. Fischinger, S., Boudreau, C.M., Butler, A.L., Streeck, H., and Alter, G. (2019). Sex differences in vaccine-induced humoral immunity. Semin. Immunopathol. *41*, 239–249. https://doi.org/10.1007/s00281-018-0726-5.

37. Kariko, K., Muramatsu, H., Ludwig, J., and Weissman, D. (2011). Generating the optimal mRNA for therapy: HPLC purification eliminates immune activation and improves translation of nucleoside-modified, protein-encoding mRNA. Nucleic Acids Res. *39*, e142. https://doi.org/10.1093/nar/gkr695.

38. Zhong, Z., McCafferty, S., Opsomer, L., Wang, H., Huysmans, H., De Temmerman, J., Lienenklaus, S., Portela Catani, J.P., Combes, F., and Sanders, N.N. (2021). Corticosteroids and cellulose purification improve, respectively, the in vivo translation and vaccination efficacy of sa-mRNAs. Mol. Ther. *29*, 1370–1381. https://doi.org/10.1016/j.ymthe.2021.01.023.

39. Zhong, Z., Portela Catani, J.P., Mc Cafferty, S., Couck, L., Van Den Broeck, W., Gorle, N., Vandenbroucke, R.E., Devriendt, B., Ulbert, S., Cnops, L., et al. (2019). Immunogenicity and protection efficacy of a naked self-replicating mRNA-based zika virus vaccine. Vaccines (Basel) *7*. https://doi.org/10.3390/vaccines7030096.

40. Stokes, A., Pion, J., Binazon, O., Laffont, B., Bigras, M., Dubois, G., Blouin, K., Young, J.K., Ringenberg, M.A., Ben Abdeljelil, N., et al. (2020). Nonclinical safety assessment of repeated administration and biodistribution of a novel rabies self-amplifying mRNA vaccine in rats. Regul. Toxicol. Pharmacol. *113*, 104648. https://doi.org/10.1016/j.yrtph.2020.104648.

41. Segal, L., Morelle, D., Kaaber, K., Destexhe, E., and Garcon, N. (2015). Non-clinical safety assessment of single and repeated intramuscular administration of a human papillomavirus-16/18 vaccine in rabbits and rats. J. Appl. Toxicol. *35*, 1577–1585. https://doi.org/10.1002/jat.3131.

42. Giordano, G., Segal, L., Prinsen, M., Wijnands, M.V., Garcon, N., and Destexhe, E. (2017). Non-clinical safety assessment of single and repeated administration of gE/AS01 zoster vaccine in rabbits. J. Appl. Toxicol. *37*, 132–141. https://doi.org/10.1002/jat.3329.

43. Huysmans, H., Zhong, Z., De Temmerman, J., Mui, B.L., Tam, Y.K., Mc Cafferty, S., Gitsels, A., Vanrompay, D., and Sanders, N.N. (2019). Expression kinetics and innate immune response after electroporation and LNP-mediated delivery of a self-amplifying mRNA in the skin. Mol. Ther. Nucleic Acids *17*, 867–878. https://doi.org/10.1016/j.omtn.2019.08.001.

44. Pollock, K.M., Cheeseman, H.M., Szubert, A.J., Libri, V., Boffito, M., Owen, D., Bern, H., O'Hara, J., McFarlane, L.R., Lemm, N., et al.. Safety and immunogenicity of a self-amplifying RNA vaccine against COVID-19: COVAC1, a phase I, dose-ranging trial. https://doi.org/10.2139/ssrn.3859294.

45. Jeffs, L.B., Palmer, L.R., Ambegia, E.G., Giesbrecht, C., Ewanick, S., and MacLachlan, I. (2005). A scalable, extrusion-free method for efficient liposomal encapsulation of plasmid DNA. Pharm. Res. *22*, 362–372. https://doi.org/10.1007/s11095-004-1873-z.

46. Lou, G., Anderluzzi, G., Schmidt, S.T., Woods, S., Gallorini, S., Brazzoli, M., Giusti, F., Ferlenghi, I., Johnson, R.N., Roberts, C.W., et al. (2020). Delivery of self-amplifying mRNA vaccines by cationic lipid nanoparticles: the impact of cationic lipid selection. J. Control. Release *325*, 370–379. https://doi.org/10.1016/j.jconrel.2020.06.027.

47. Ragan, I.K., Hartson, L.M., Dutt, T.S., Obregon-Henao, A., Maison, R.M., Gordy, P., Fox, A., Karger, B.R., Cross, S.T., Kapuscinski, M.L., et al. (2021). A whole virion vaccine for COVID-19 produced via a novel inactivation method and preliminary demonstration of efficacy in an animal challenge model. Vaccines (Basel) *9*. https://doi.org/10.3390/vaccines9040340.

48. WHO (2005). WHO guidelines on nonclinical evaluation of vaccines. https://www.who.int/biologicals/publications/trs/areas/vaccines/nonclinical_evaluation/ANNEX%201Nonclinical.P31-63.pdf.

49. FGF Industry (2007). Considerations for plasmid DNA vaccines for infectious disease indications. https://www.fda.gov/files/vaccines,%20blood%20&%20biologics/published/Guidance-for-Industry–Considerations-for-Plasmid-DNA-Vaccines-for-Infectious-Disease-Indications.pdf.

YMTHE, Volume *30*

Supplemental Information

A self-amplifying mRNA SARS-CoV-2 vaccine candidate induces safe and robust protective immunity in preclinical models

Giulietta Maruggi, Corey P. Mallett, Jason W. Westerbeck, Tiffany Chen, Giuseppe Lofano, Kristian Friedrich, Lin Qu, Jennifer Tong Sun, Josie McAuliffe, Amey Kanitkar, Kathryn T. Arrildt, Kai-Fen Wang, Ian McBee, Deborah McCoy, Rebecca Terry, Alison Rowles, Maia Araujo Abrahim, Michael A. Ringenberg, Malcolm J. Gains, Catherine Spickler, Xuping Xie, Jing Zou, Pei-Yong Shi, Taru Dutt, Marcela Henao-Tamayo, Izabela Ragan, Richard A. Bowen, Russell Johnson, Sandra Nuti, Kate Luisi, Jeffrey B. Ulmer, Ann-Muriel Steff, Rashmi Jalah, Sylvie Bertholet, Alan H. Stokes, and Dong Yu

SUPPLEMENTAL FIGURES AND LEGENDS

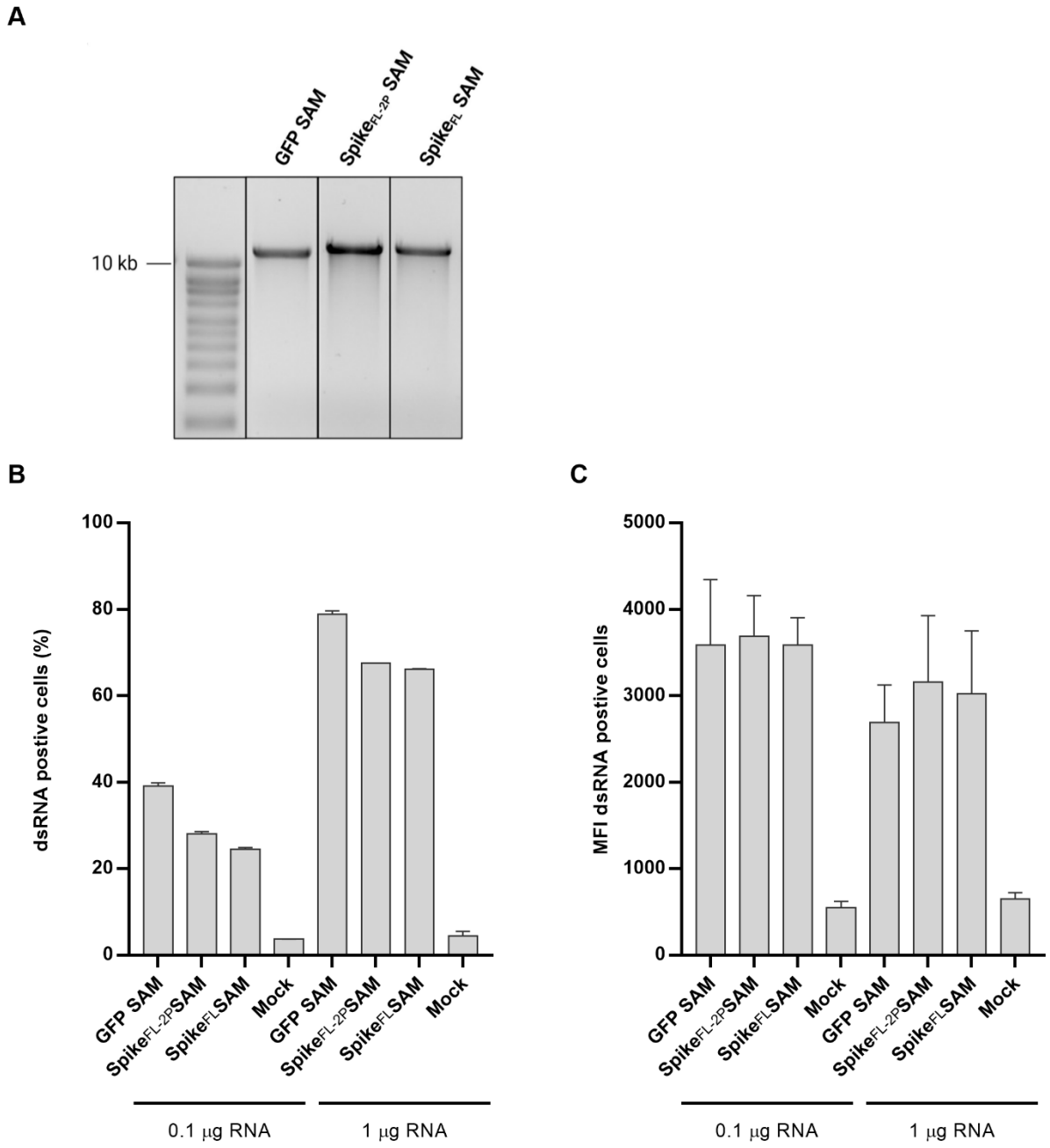

Figure S1. SARS-CoV-2 SAM *in vitro* characterization. (**A**) Quality of GFP and SARS-CoV-2 SAM RNA as measured by denaturing RNA agarose gel electrophoresis. (**B, C**) *In vitro* potency of SARS-CoV-2 SAM electroporated RNAs in BHK cells, as measured by (**B**) the percentage of double-stranded RNA (dsRNA) positive cells and (**C**) mean fluorescence intensity (MFI) by flow cytometry using an anti-dsRNA antibody. Mock, mock transfected cells; GFP, green fluorescent protein; $Spike_{FL-2P}$, prefusion stabilized spike sequence; $Spike_{FL}$, wild type full length spike sequence.

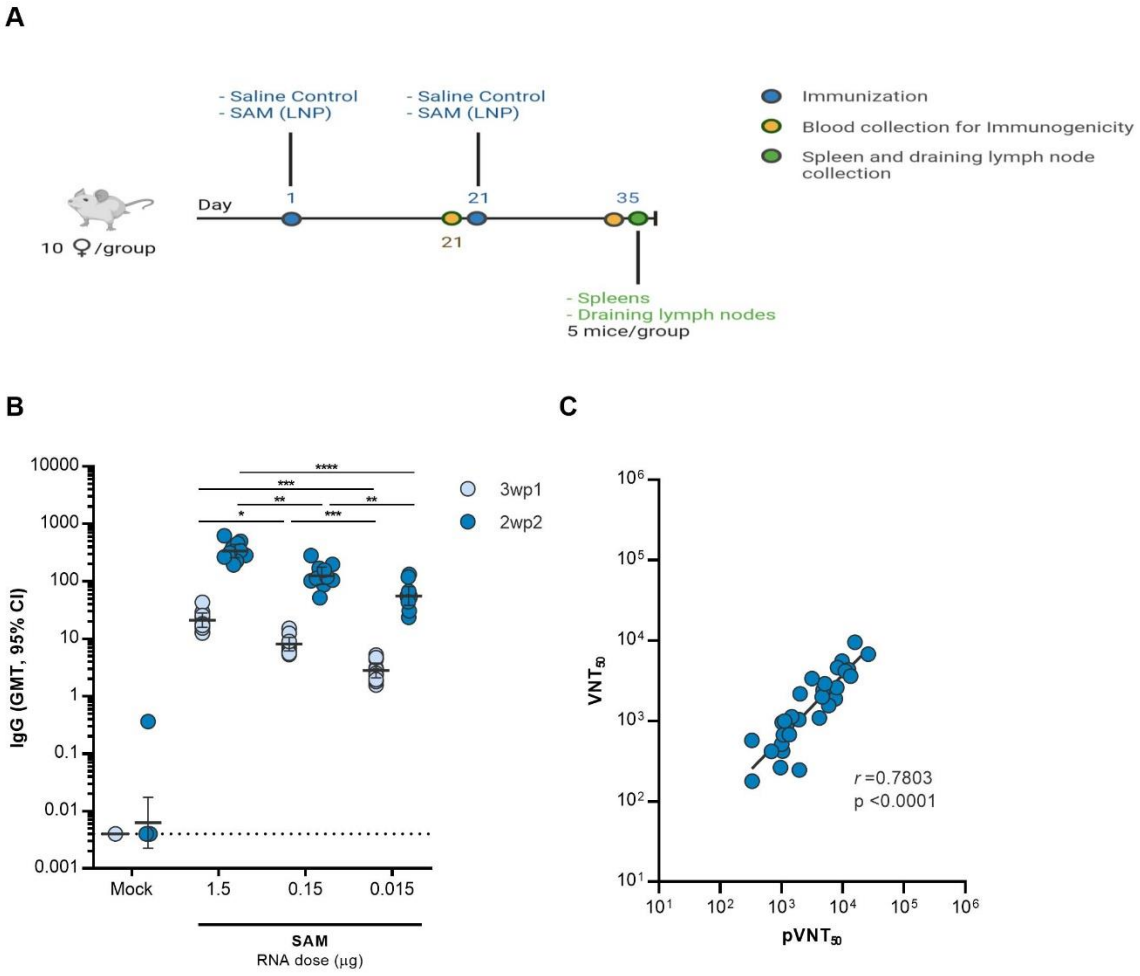

Figure S2. Mouse immunogenicity study design and humoral responses elicited by SARS-CoV-2 SAM (LNP) vaccine. (A) Study design. Female BALB/c mice (10 per group) were immunized intramuscularly (i.m.) with SARS-CoV-2 SAM (LNP) vaccine at a dose of 1.5 μg, 0.15 μg or 0.015 μg, or of saline as mock control. Sera were collected at Days 21 and 35 from all mice to measure binding and neutralizing antibody titers. At Day 35 spleens and draining inguinal lymph nodes were collected from 5 mice/group to characterize Spike-specific B cell and $CD4^+$ and $CD8^+$ T cell responses. **(B)** SARS-CoV-2 Spike-specific IgG binding antibody titers in sera collected 3 weeks after the first (3wp1) and 2 weeks after the second administration (2wp2) from mice immunized with SAM vaccine or saline control, as determined by a Luminex-based assay. Dots represent individual mice. The dotted line indicates the limit of detection. Geometric means (GMT) of each group ± 95% confidence interval (CI) are shown. Bars indicate significant differences between groups with *p* values marked by asterisks as *, $p < 0.05$; **, $p < 0.01$; ***, $p < 0.001$; ****, $p < 0.0001$. Responses in sera collected 2wp2 from SAM vaccinated mice were significantly higher than those collected from the mock group. (**C**) Pearson correlation of VSV-SARS-CoV-2 pVNT50 (shown in Figure 2A) and live SARS-CoV-2 VNT_{50} from 30 mice (10 mice/dose group) immunized with SAM and collected at 2wp2.

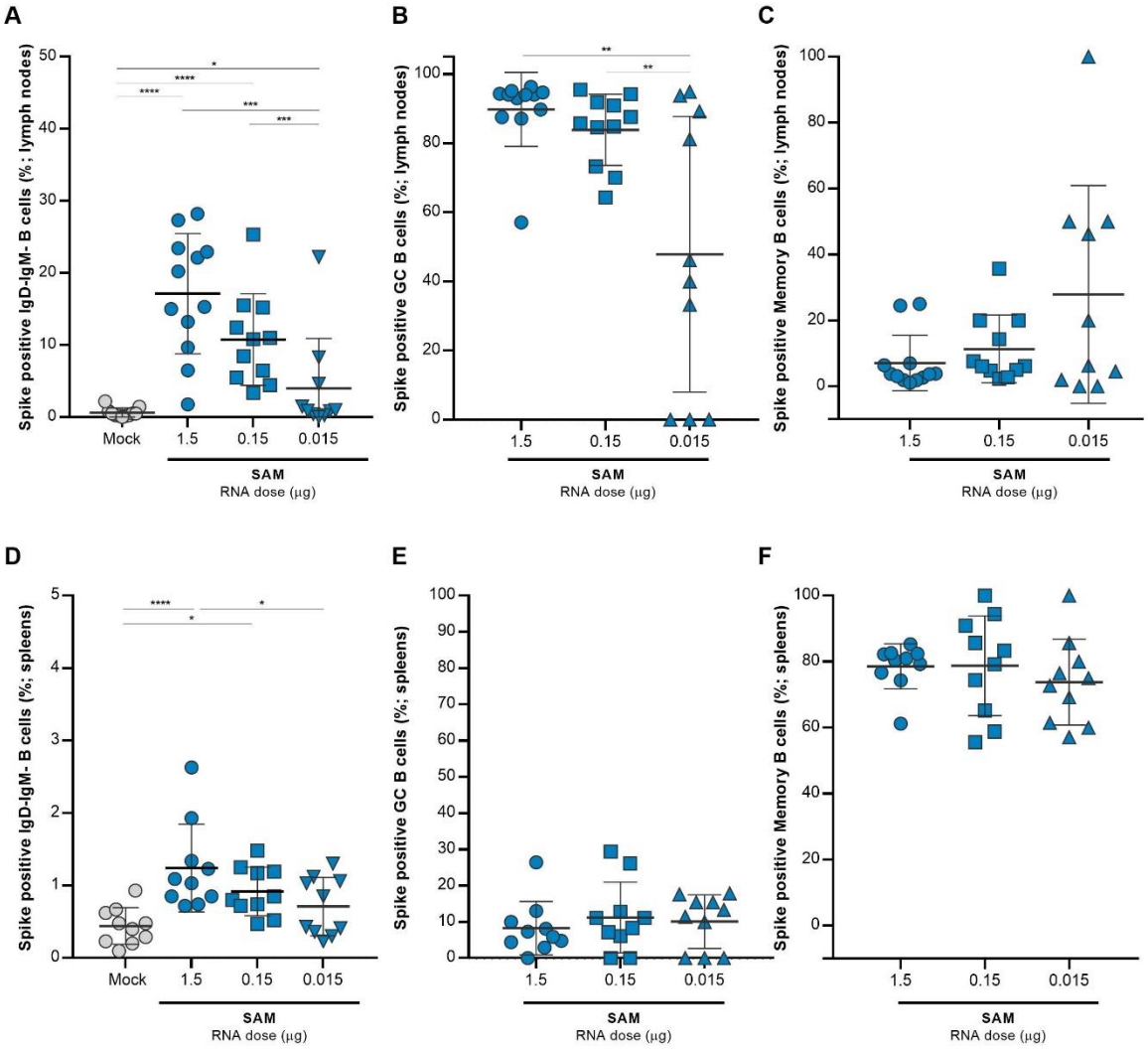

Figure S3. Spike-specific germinal center (GC) and memory B cell responses in inguinal draining lymph nodes and spleens of mice immunized with SARS-CoV-2 SAM (LNP) vaccine. Inguinal draining lymph nodes (**A-C**) and spleens (**D-F**) of immunized mice were harvested 2wp2 and analyzed for frequency of SARS-CoV-2 Spike-specific class switched B cells (defined as live $CD3^-CD19^+IgM^-IgD^-Spike^-AF488^+$) (**A, D**); frequency of Spike-specific GC B cells (defined as live $CD3^-CD19^+IgD^-IgM^-Spike\text{-}AF488^+CD95^+GL7^+$ cells) (**B, E**), and frequency of Spike-specific memory B cells (defined as live $CD3^-CD19^+IgD^-IgM^-Spike\text{-}AF488^+CD95^-CD38^+$) cells (**C, F**). Data are combined from two independent experiments at 2wp2 (5 mice/group/experiment). Means ± standard deviation (SD) for each group are shown, and each data point represents an individual mouse. Bars indicate significant differences between groups with *p* values marked by asterisks as *, $p < 0.05$; **, $p < 0.01$; ***, $p < 0.001$; ****, $p < 0.0001$.

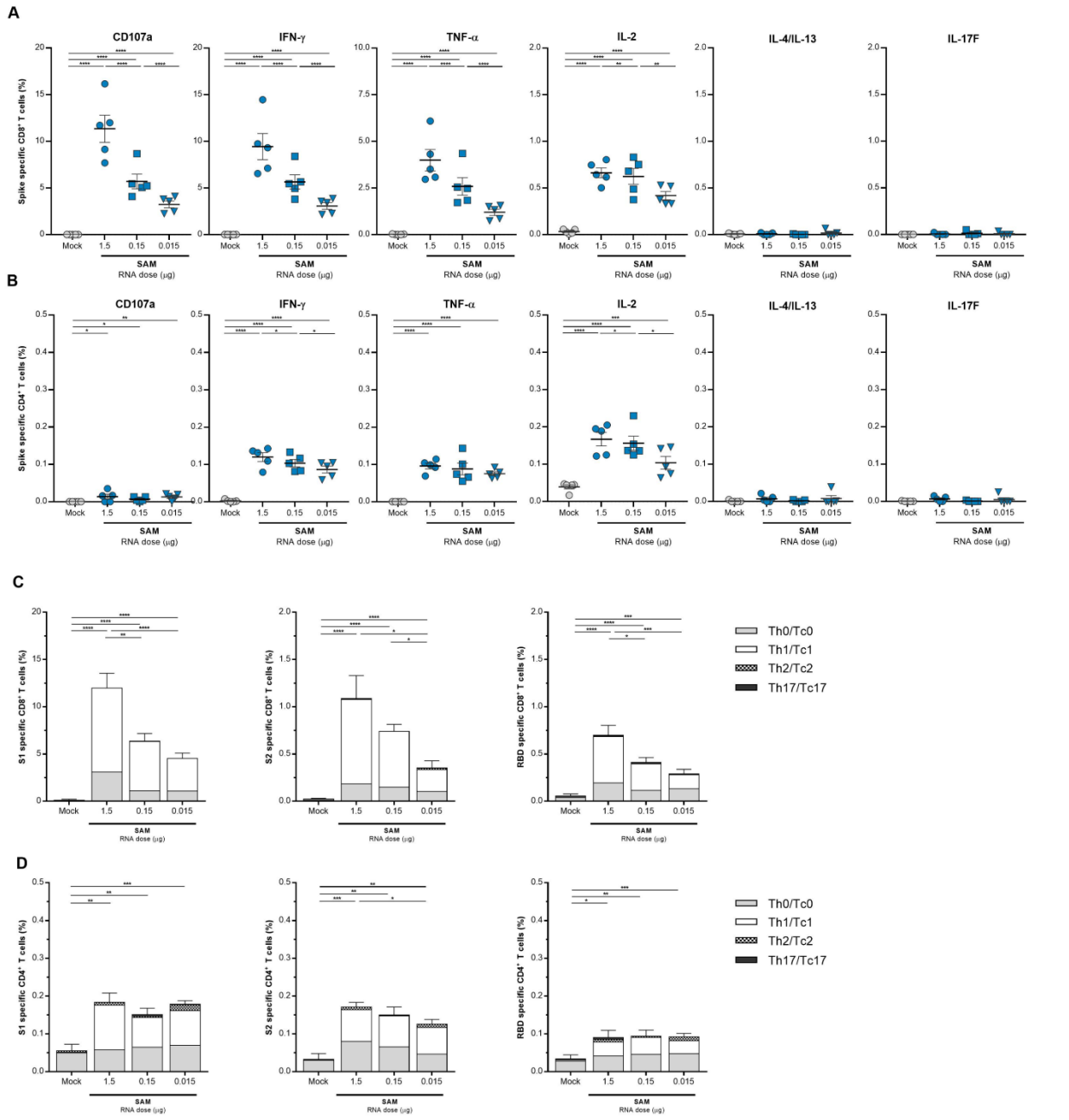

Figure S4. Spike-specific T cell responses induced by SARS-CoV-2 SAM (LNP) vaccine in mice. $Spike_{FL\text{-}2P}$-specific $CD8^+CD44^+$ (**A**) and $CD4^+CD44^+$ (**B**) T cell cytokines from splenocytes of individual immunized mice, as measured by flow cytometry at 2wp2. (**C, D**) S1, S2 or RBD specific T cell responses measured by flow cytometry after *ex vivo* stimulation of splenocytes harvested from immunized mice at 2wp2. The stacked bars (**C, D**) indicate distribution of the Tc0/Tc1/Tc2/Tc17 cytotoxic cells within the total $CD8^+$ (**C**) and the Th0/Th1/Th2/Th17 T helper cells within the $CD4^+$ (**D**) Spike-specific T cells (Mean ± standard error of mean (SEM)). Bars indicate significant differences between groups with *p* values marked by asterisks as *, $p < 0.05$; **, $p < 0.01$; ***, $p < 0.001$; ****, $p < 0.0001$.

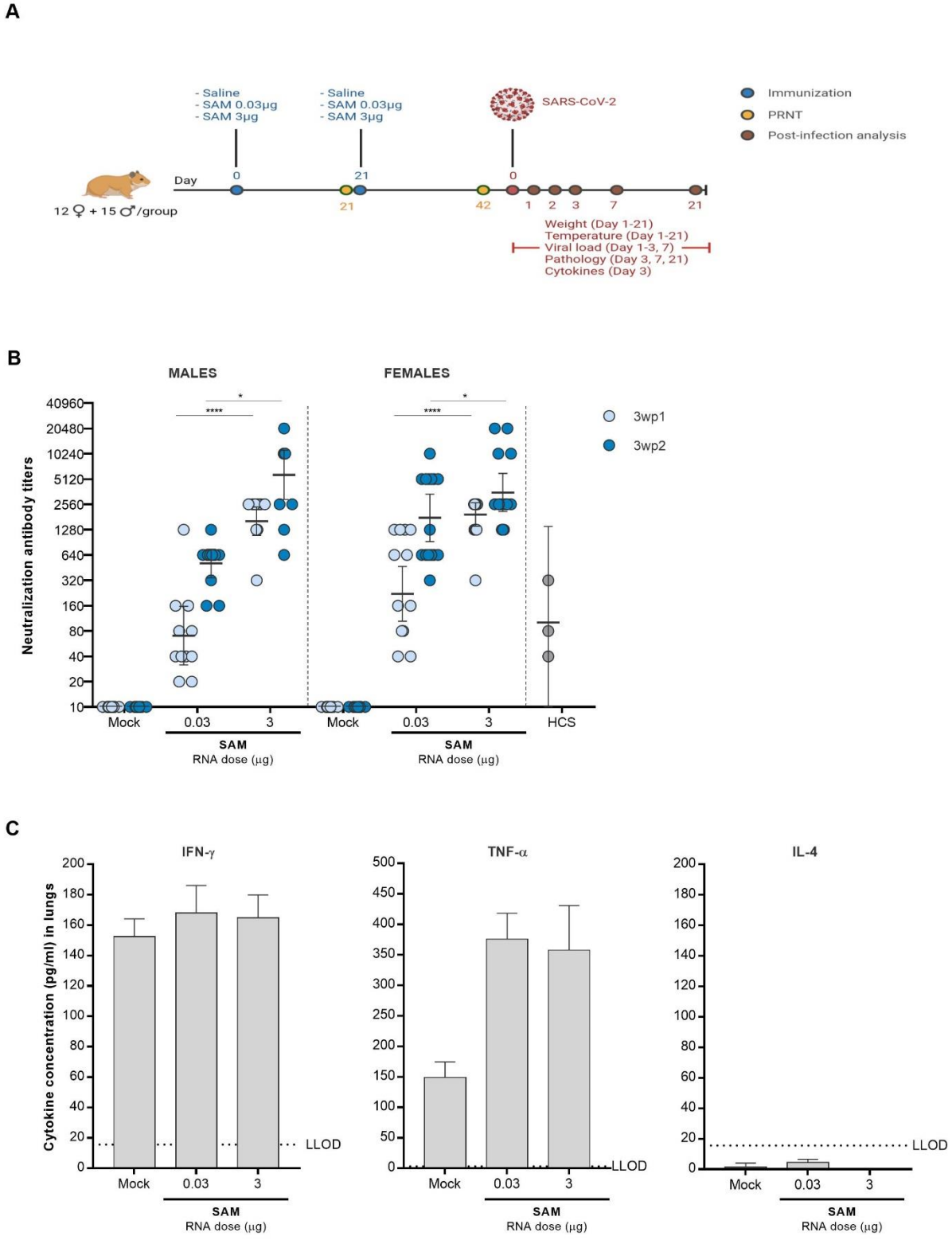

Figure S5. Immunogenicity and efficacy of SARS-CoV-2 SAM (LNP) vaccine candidate in hamsters. (A) Study design. Male and female Golden Syrian hamsters were injected i.m. with 0.03µg or 3 µg of SARS-CoV-2 SAM (LNP) vaccine or with saline (mock) at Days 0 and 21. Sera were collected at Day 21 (3wp1) and 42 (3wp2) to measure neutralizing antibody titers. At Day 42, animals were challenged intranasally with SARS-CoV-2 (isolate USA-

WA1/2020) (10^4 PFU) under BSL-3 containment level. At 1, 2, 3, 7, and 21 dpi hamsters (n=8 per group) were euthanized for tissue collection. **(B)** Serum SARS-CoV-2 neutralizing antibody titers as measured by plaque reduction neutralization assay (PRNT). Neutralizing antibody titers were compared to a panel of COVID-19 human convalescent sera (HCS; n=3) samples. Bars denote GMT±95% CI. **(C)** Analysis of cytokines in the supernatants from dissociated lung cells collected at 3 dpi and cultured without stimulation. Bars denote group means ± SD. Horizontal dotted line denotes lower limit of detection (LLOD).

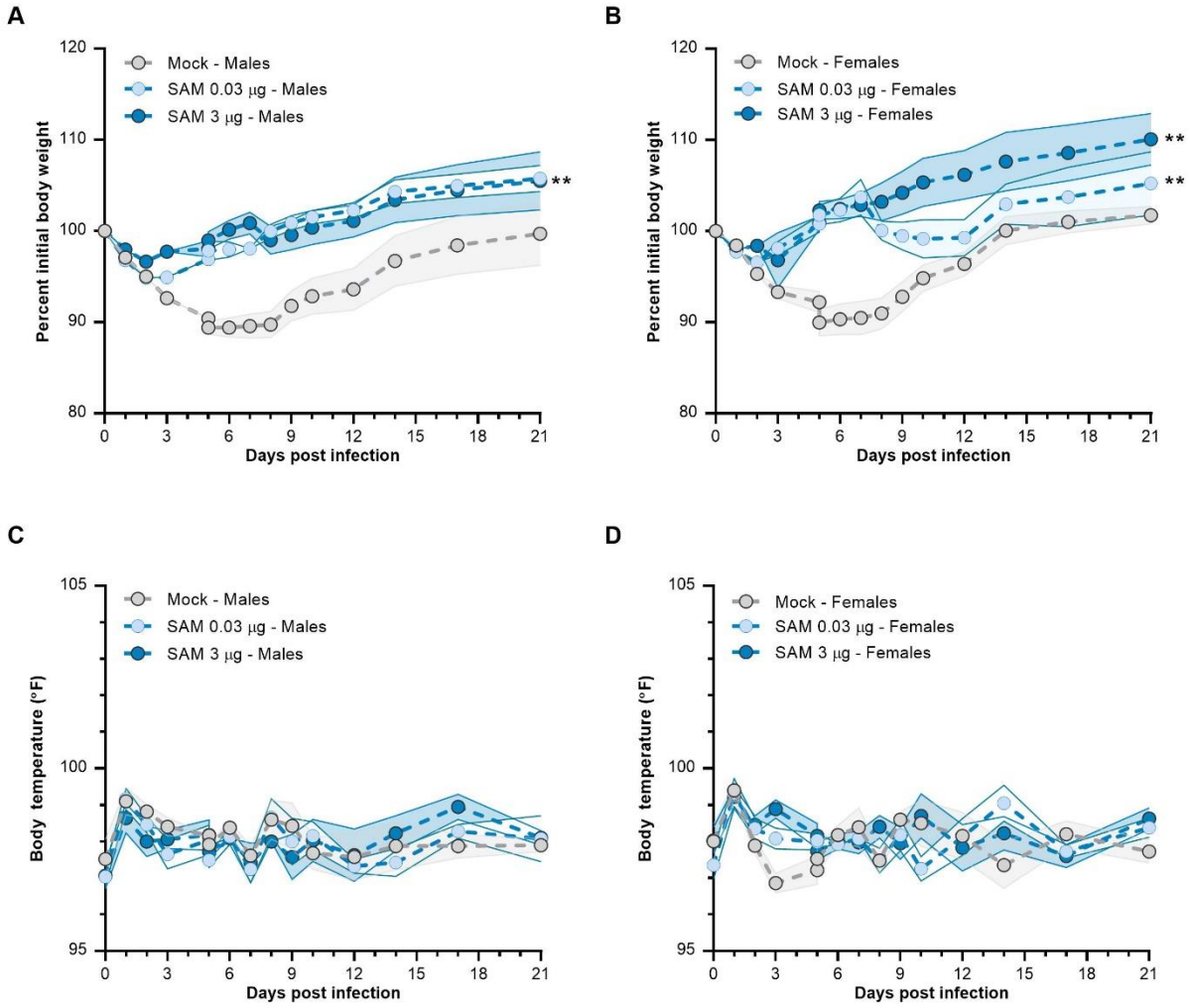

Figure S6. Weight and body temperature changes following SARS-CoV-2 challenge of vaccinated hamsters. (**A-B**) Percent weight change in male (**A**) and female (**B**) animals over 21 days post infection. Mean weights are highlighted by colored symbols. Shaded area represents SEM. **, $p < 0.01$, as compared to the mock vaccinated animals. (**C-D)** Body temperature measured daily in male (**C**) and female (**D**) animals over 21 days post infection. Mean temperature are highlighted by color symbols. Shaded area represents SEM.

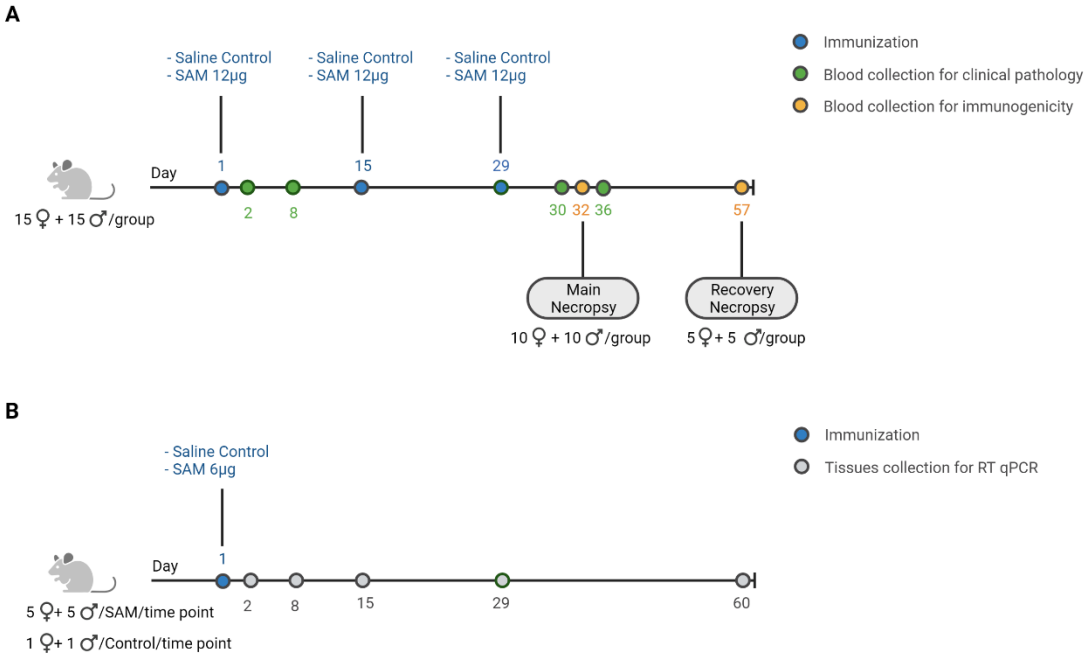

Figure S7. Repeated-dose toxicology and biodistribution experimental design. **(A)** Repeated dose study. Male and female Sprague-Dawley rats were injected i.m. on Day 1, 15, and 29 with either SARS-CoV-2 SAM (LNP) or saline. Ten animals/sex/group constituted the main study group, necropsied at Day 32, and 5 animals/sex/group were in the recovery group, necropsied at Day 57. **(B)** Biodistribution study. Male and female Sprague-Dawley rats were injected once with either SARS-CoV-2 SAM (LNP) or saline. The treated group was divided in 5 subgroups of 10 animals (n=5/sex) and the control group was divided in 5 subgroups of 2 animals (n=1/sex). Each subgroup corresponded to the 5 time points of necropsy where organs were collected for RT-qPCR analysis.

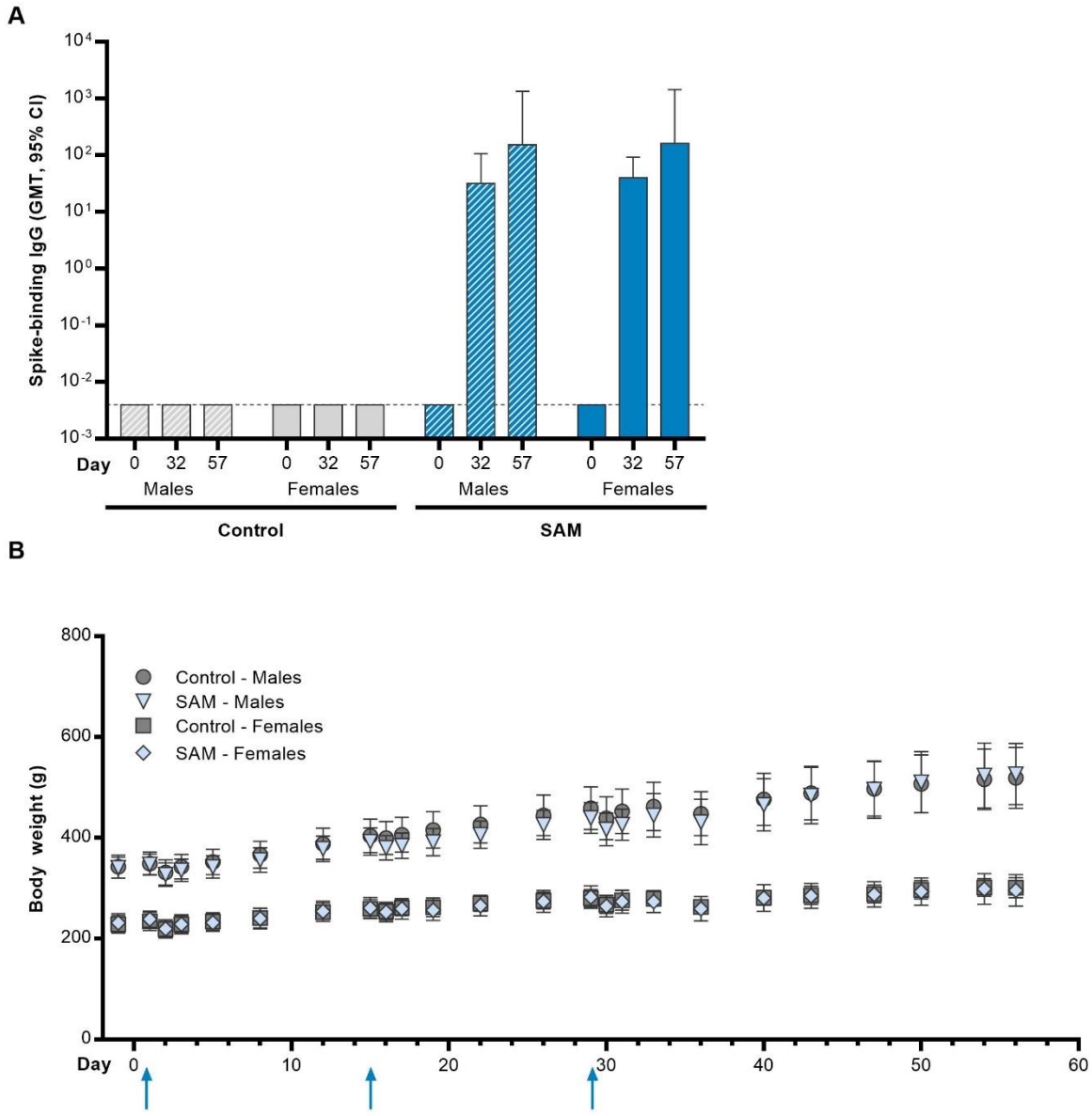

Figure S8. Rat immune responses and body weight changes after SARS-CoV-2 SAM (LNP) vaccination. (A) Spike-specific antibody (IgG) titers were measured in the sera of rats prior to immunization (Day 0), 3 days (Day 32), and 28 days (Day 57) following the third immunization. The graph shows GMT±95% CI. (**B**) The body weights were measured at multiple time points during the 57 days of the study. The graph shows mean body weights with SD. Arrows indicate the vaccine administration.

Table S1. Repeated-dose study. Effect of SARS-CoV-2 SAM (LNP) injection on selected clinical pathology parameters in male Sprague-Dawley rats.

	Day 2		Day 8		Day 30		Day 36		Day 57	
	Control	SAM	Control	SAM	Control	SAM	Control	SAM	Control	SAM
White blood cells [× 10^9/L]	9.724 (1.782)	10.461 (2.277)	9.602 (0.904)	10.828 (1.674)	10.210 (1.682)	**14.334 (3.402) ****	8.818 (0.944)	11.124 (2.030)	7.792 (1.933)	8.626 (1.854)
Neutrophils [× 10^9/L]	1.154 (0.330)	**7.691 (1.747) *****	1.454 (0.293)	1.848 (0.825)	1.732 (0.329)	**10.223 (4.893) *****	1.558 (0.430)	1.978 (0.527)	1.662 (0.597)	1.808 (0.845)
Lymphocytes [× 10^9/L]	8.165 (1.501)	**2.443 (0.661) *****	7.744 (0.768)	8.465 (1.485)	8.373 (1.337)	**3.590 (2.639) ****	6.770 (0.915)	8.590 (1.982)	5.720 (1.754)	6.358 (1.380)
Monocytes [× 10^9/L]	0.209 (0.099)	0.161 (0.070)	0.178 (0.048)	0.268 (0.138)	0.217 (0.075)	0.236 (0.104)	0.250 (0.037)	0.264 (0.123)	0.192 (0.086)	0.256 (0.127)
Eosinophils [× 10^9/L]	0.072 (0.030)	0.068 (0.023)	0.104 (0.051)	0.110 (0.018)	0.114 (0.052)	0.161 (0.110)	0.142 (0.060)	0.162 (0.059)	0.142 (0.056)	0.108 (0.042)
Basophils [× 10^9/L]	0.054 (0.013)	**0.031 (0.012) ****	0.062 (0.013)	0.055 (0.006)	0.062 (0.014)	0.048 (0.022)	0.032 (0.004)	**0.048 (0.015) ***	0.034 (0.023)	0.038 (0.004)
Red blood cells [× 10^{12}/L]	8.173 (0.618)	8.525 (0.331)	8.614 (0.280)	**7.573 (0.486) ****	8.929 (0.398)	8.475 (0.885)	8.338 (0.859)	8.120 (0.859)	8.534 (0.516)	9.056 (0.436)
Hemoglobin [g/L]	158.8 (7.2)	163.6 (6.4)	168.6 (2.9)	**143.3 (12.6) ****	161.8 (4.1)	152.8 (16.3)	154.2 (12.0)	148.0 (10.7)	154.4 (14.9)	164.8 (8.9)
Hematocrit [L/L]	0.464 (0.023)	0.479 (0.020)	0.486 (0.009)	**0.428 (0.038) ***	0.476 (0.014)	0.442 (0.051)	0.438 (0.036)	0.428 (0.030)	0.456 (0.044)	0.494 (0.027)
Fibrinogen [g/L]	2.79 (0.73)	**6.89 (0.50) *****	3.21 (0.24)	3.27 (0.55)	3.45 (0.69)	**4.47 (1.42) ***	3.04 (0.33)	**3.79 (0.60) ***	3.24 (0.36)	3.16 (0.38)
AST [U/L]	133.2 (22.9)	137.9 (30.6)	116.4 (12.5)	**158.8 (24.7) ****	173.1 (50.7)	165.7 (20.7)	114.6 (26.6)	115.2 (10.1)	114.6 (24.0)	129.6 (23.4)
ALT [U/L]	44.7 (6.2)	45.1 (3.0)	57.4 (11.5)	56.6 (6.5)	55.0 (14.9)	57.7 (5.8)	48.0 (9.2)	44.8 (5.4)	47.2 (8.0)	43.0 (6.4)
ALP [U/L]	250.9 (75.8)	243.8 (52.5)	239.8 (17.0)	284.6 (40.3)	165.4 (40.1)	174.4 (32.1)	151.8 (11.3)	168.6 (30.8)	130.4 (19.5)	135.8 (14.0)
Albumin [g/L]	45.2 (2.49)	**40.65 (1.05) *****	46.36 (1.62)	**43.90 (0.64) ***	45.37 (2.23)	**39.15 (1.69) *****	45.06 (1.29)	**39.82 (2.08) ****	45.76 (3.19)	44.76 (1.24)
Globulin [g/L]	17.7 (1.40)	**23.15 (1.82) *****	19.66 (1.65)	19.20 (1.97)	21.83 (1.06)	**25.42 (1.87) *****	20.96 (1.45)	19.40 (2.51)	23.88 (3.42)	21.16 (2.37)
Albumin/ Globulin ratio	2.653 (0.232)	**1.765 (0.146) *****	2.370 (0.204)	2.304 (0.223)	1.992 (0.157)	**1.548 (0.131) *****	2.154 (0.106)	2.084 (0.339)	2.022 (0.201)	2.134 (0.222)

All values are means (SD). Statistically significant differences are shown in bold. AST, aspartate aminotransferase; ALT, alanine aminotransferase; ALP, alkaline phosphatase. *, $p < 0.05$; **, $p < 0.01$; ***, $p < 0.001$, compared with control.

Table S2. Repeated-dose study. Effect of SARS-CoV-2 SAM (LNP) injection on selected clinical pathology parameters in female Sprague-Dawley rats.

	Day 2		**Day 8**		**Day 30**		**Day 36**		**Day 57**	
	Control	SAM	Control	SAM	Control	SAM	Control	SAM	Control	SAM
White blood cells [× 10^9/L]	8.882 (2.375)	9.026 (2.360)	8.903 (2.415)	9.446 (3.882)	8.922 (2.514)	10.177 (2.155)	8.338 (2.533)	10.186 (4.993)	6.150 (3.129)	6.534 (2.294)
Neutrophils [× 10^9/L]	0.800 (0.413)	**5.451 (0.953) *****	0.913 (0.148)	1.330 (0.919)	0.795 (0.390)	**6.336 (1.975) *****	1.215 (0.342)	1.226 (0.760)	1.006 (0.517)	0.698 (0.209)
Lymphocytes [× 10^9/L]	7.689 (2.106)	**3.253 (1.762) *****	7.585 (2.228)	7.674 (2.994)	7.719 (2.456)	**3.463 (1.397) *****	6.716 (2.096)	8.472 (4.699)	4.824 (3.116)	5.540 (2.035)
Monocytes [× 10^9/L]	0.184 (0.059)	**0.123 (0.069) ***	0.213 (0.116)	0.184 (0.083)	0.186 (0.068)	0.159 (0.118)	0.183 (0.062)	0.206 (0.135)	0.150 (0.051)	0.140 (0.053)
Eosinophils [× 10^9/L]	0.104 (0.036)	0.119 (0.042)	0.093 (0.081)	0.136 (0.050)	0.100 (0.037)	0.119 (0.052)	0.115 (0.066)	0.132 (0.064)	0.090 (0.068)	0.080 (0.032)
Basophils [× 10^9/L]	0.037 (0.014)	0.027 (0.012)	0.040 (0.008)	0.044 (0.023)	0.048 (0.022)	0.047 (0.042)	0.040 (0.022)	0.042 (0.026)	0.028 (0.019)	0.026 (0.011)
Red blood cells [× 10^{12}/L]	7.769 (0.546)	7.772 (0.589)	7.960 (0.449)	7.652 (0.320)	8.101 (0.393)	7.974 (0.872)	7.783 (0.706	7.860 (0.299)	7.458 (1.378)	8.244 (0.536)
Hemoglobin [g/L]	149.3 (11.1)	150.8 (11.3)	154.3 (10.2)	147.0 (7.5)	154.6 (7.5)	153.5 (15.6)	151.8 (11.8)	151.8 (6.5)	145.2 (26.9)	160.4 (5.4)
Hematocrit [L/L]	0.426 (0.029)	0.431 (0.033)	0.440 (0.027)	0.422 (0.011)	0.444 (0.023)	0.444 (0.048)	0.428 (0.034)	0.426 (0.017)	0.420 (0.080)	0.470 (0.014)
Fibrinogen [g/L]	2.59 (0.13)	**6.40 (0.54) *****	2.69 (0.22)	2.32 (1.32)	2.31 (0.33)	**4.59 (0.64) *****	2.45 (0.17)	2.45 (0.47)	2.14 (0.39)	2.27 (0.06)
AST [U/L]	123.8 (25.5)	**162.0 (52.5) ***	126.8 (23.5)	161.0 (38.7)	126.1 (26.4)	**297.3 (407.0) ***	100.8 (17.7)	109.4 (27.7)	140.2 (28.5)	118.0 (33.5)
ALT [U/L]	37.6 (7.3)	74.0 (17.4)	44.0 (4.7)	65.6 (37.0)	52.1 (10.1)	114.0 (144.1)	48.4 (7.8)	43.8 (10.8)	52.6 (14.3)	51.4 (23.9)
ALP [U/L]	129.9 (23.0)	117.8 (18.8)	129.3 (25.3)	127.4 (24.2)	81.3 (17.3)	90.9 (20.1)	67.4 (13.0)	75.8 (16.7)	54.8 (18.1)	56.4 (10.0)
Albumin [g/L]	51.97 (2.28)	**47.44 (4.46) ****	53.53 (1.21)	**48.18 (2.49) ****	53.74 (2.42)	**48.49 (5.23) ****	56.02 (1.99)	**47.88 (3.28) ****	56.22 (2.99)	55.58 (2.52)
Globulin [g/L]	16.11 (2.30)	**20.12 (1.14) *****	15.95 (0.85)	17.46 (1.21)	19.98 (1.80)	21.55 (2.44)	17.60 (2.58)	17.90 (2.19)	17.18 (2.72)	19.22 (2.27)
Albumin/ Globulin ratio	3.271 (0.362)	**2.364 (0.259) *****	2.363 (0.223)	**2.766 (0.210) ****	2.703 (0.189)	**2.259 (0.185) ****	3.236 (0.454)	**2.694 (0.217) ***	3.334 (0.482)	2.926 (0.385)

All values are means (SD). Statistically significant differences are shown in bold. AST, aspartate aminotransferase; ALT, alanine aminotransferase; ALP, alkaline phosphatase. *, $p < 0.05$; **, $p < 0.01$; ***, $p < 0.001$, compared with control.

Table S3. Repeated-dose study. Mean absolute, relative-to-body and relative-to-brain weights of selected lymph nodes and spleens in control and SARS-CoV-2 SAM (LNP)-treated rats.

	Main (Day 32)				Recovery (Day 57)			
	Males (n=10)		Females (n=10)		Males (n=5)		Females (n=5)	
	Control	SAM	Control	SAM	Control	SAM	Control	SAM
Iliac lymph node								
Absolute [g]	0.03209 (0.01109)	0.04974 (0.02782)	0.02726 (0.01022)	**0.03966 (0.01497)***	0.03794 (0.01650)	0.03684 (0.00780)	0.03172 (0.00972)	0.02138 (0.01097)
Relative to body weight [%]	0.00751 (0.00273)	0.01230 (0.00659)	0.01052 (0.00414)	**0.01545 (0.00598)***	0.00782 (0.00394)	0.00725 (0.00082)	0.01094 (0.00272)	0.00784 (0.00445)
Relative to brain weight [%]	1.49067 (0.49993)	2.36712 (1.31305)	1.37129 (0.52016)	**1.98901 (0.74210)***	1.69281 (0.74787)	1.66112 (0.29990)	1.55610 (0.47545)	1.04615 (0.56875)
Popliteal lymph node								
Absolute [g]	0.04953 (0.03412)	0.04962 (0.01440)	0.02469 (0.00668)	**0.03614 (0.01255)***	0.02572 (0.00652)	0.02172 (0.00839)	0.01660 (0.00675)	0.02066 (0.00696)
Relative to body weight [%]	0.01146 (0.00750)	0.01240 (0.00365)	0.00953 (0.00262)	**0.01393 (0.00438)***	0.00522 (0.00131)	0.00426 (0.00152)	0.00580 (0.00249)	0.00750 (0.00289)
Relative to brain weight [%]	2.33749 (1.67971)	2.36011 (0.67201)	1.23894 (0.34208)	**1.81346 (0.59482)***	1.14765 (0.29757)	0.97799 (0.36840)	0.81281 (0.32381)	1.00206 (0.34223)
Inguinal lymph node								
Absolute [g]	0.05122 (0.02257)	0.04930 (0.01350)	0.03509 (0.02477)	0.05173 (0.03941)	0.02370 (0.01440)	0.03278 (0.01681)	0.02046 (0.00446)	0.02398 (0.00501)
Relative to body weight [%]	0.01190 (0.00500)	0.01224 (0.00309)	0.01322 (0.00873)	0.02002 (0.01497)	0.00463 (0.00246)	0.00639 (0.00288)	0.00713 (0.00150)	0.00866 (0.00220)
Relative to brain weight [%]	2.38723 (1.04494)	2.35144 (0.66499)	1.74379 (1.19519)	2.59969 (1.94192)	1.04118 (0.60265)	1.46450 (0.70299)	1.00289 (0.21710)	1.16150 (0.24581)
Spleen								
Absolute [g]	0.78034 (0.09648)	**0.95305 (0.17387)***	0.54410 (0.04282)	**0.66476 (0.13521)***	0.76534 (0.12726)	0.78698 (0.14753)	0.48404 (0.12677)	0.56048 (0.11678)
Relative to body weight [%]	0.18373 (0.01439)	**0.23739 (0.04064)****	0.20930 (0.02012)	**0.25764 (0.04400)****	0.15549 (0.02262)	0.15594 (0.02502)	0.16807 (0.03831)	0.19938 (0.03611)
Relative to brain weight [%]	36.52873 (4.03627)	**45.36674 (8.08238)***	27.29450 (1.86765)	**33.39376 (6.32573)***	34.09256 (5.03680)	35.65214 (6.65324)	23.82166 (6.73888)	27.09681 (5.47487)

All values are means (SD). Statistically significant differences are shown in bold. *, $p < 0.05$; **, $p < 0.01$; ***, $p < 0.001$, compared with control.

SUPPLEMENTAL METHODS

SARS-CoV-2 SAM synthesis

In vitro RNA transcription and purification was performed as previously described[6]. Briefly, DNA plasmids encoding the RNA SAM vaccines sequence were linearized by restriction digestion with BspQI at the precise 3′ end of the SAM sequences and purified by phenol-chloroform extraction. Linearized DNA templates were in vitro transcribed using T7 RNA polymerase (NEB) and subsequently capped using a vaccinia capping enzyme (NEB). Denaturing agarose gel electrophoresis was performed to evaluate the integrity of the RNA as previously described.[6]

LNP formulation preparation

LNP encapsulating SAM were prepared through flash precipitation by mixing an ethanolic solution of lipids with an aqueous solution of RNA as described previously.[45] Lipid excipient components (proprietary ionizable lipid, 1,2-distearoyl-sn-glycero-3-phosphocholine (DSPC), cholesterol and 1,2-dimyristoyl-sn-glycero-3-phosphoethanolamine-N-[methoxy(polyethylene glycol)-2000] (DMPE-PEG2000)) were dissolved in ethanol at mole ratio of 40:10:48:2[6]. SAM was in a citrate buffer solution at pH 6.0. The lipid mixture was rapidly mixed with SAM in a microfluidic mixing chip at a flow rate of 1:2, respectively, using a NanoAssemblr Benchtop System (Precision Nanosystems, Vancouver BC, Canada). The formed nanoparticles were held briefly at room temperature (RT) and then transferred to a Tris-buffered solution. Concentration of SAM (LNP) was adjusted to target concentrations by dilution. Analytical characterization included size and polydispersity determination (Zetasizer DLS, Malvern Instruments), appearance, pH, osmolality, RNA concentration and entrapment by fluorometric assay using Ribogreen RNA dye, endotoxin content by LAL assay, and lipid identity and composition by HPLC. All LNP prepared had a hydrodynamic radius of less than 120 nm, and mRNA entrapment of greater than 80% as determined by Ribogreen assay (as described in [6,46]). Final materials were aseptically transferred into glass vials, stoppered, capped and frozen at -80 ± 10°C.

IN VITRO CHARACTERIZATION OF SAM CONSTRUCTS

RNA potency assay and intracellular protein expression

To determine the efficiency of SAM to launch the self-amplification cycle, approximately 1×10^6 Baby Hamster Kidney (BHK) or C2C12 mouse myoblast cells were electroporated (one pulse, 120 V, 25 milliseconds (ms)) with 0.1 µg or 1µg of SAM respectively, together with mouse thymus carrier RNA (Takara) up to 4.2 µg total RNA. Cells were seeded in six-well plates in DMEM medium containing 1% fetal bovine serum (FBS) and Penicillin–Streptomycin (P/S) and incubated at 37°C and 5% CO_2 for 18 hours. Cells were collected, fixed, permeabilized with Cytofix/Cytoperm (BD Biosciences) and then stained with allophycocyanin (APC) (Zenon Allophycocyanin Labeling Kit, Invitrogen) conjugated anti-dsRNA antibody (J2 monoclonal IgG2a antibody, Bioclass) or with an anti-S2 antibody (1A9 mouse monoclonal IgG1, GeneTex) followed by a goat anti-mouse IgG Alexa 488 secondary antibody (Invitrogen). Cells were acquired on a Fortessa X20 SORP flow cytometer (BD Biosciences) and analyzed by FlowJo v10 software (FlowJo, BD Biosciences).

Immunoblot analysis

Approximately 1×10^6 BHK cells were electroporated (one pulse, 120 V, 25 ms) with 1.0 µg of SAM together with mouse thymus carrier RNA (Takara) up to 4.2 µg total RNA. Cells were seeded in six-well plates in DMEM containing 1% FBS and P/S. At 18 hours after electroporation, cells were lysed under nonreducing conditions and whole-cell lysates subjected to SDS–polyacrylamide gel electrophoresis and blotted to a nitrocellulose membrane using a semi-dry transfer system (ThermoFisher). A recombinant Spike protein (Acro Biosystems) was loaded as control. SARS-CoV-2 Spike and actin proteins were detected using the mouse anti-S2 antibody (1A9 mouse monoclonal IgG1, GeneTex) and rabbit anti-actin antibody (Millipore) at a dilution of 1:1,000, followed by IRDye 800CW–conjugated donkey anti-mouse IgG secondary and IRDye 680RD Goat anti-Rabbit antibody (LI-COR) at a 1:15,000 dilution. Protein bands were visualized on the Odyssey fluorescent imager (LI-COR).

Flow cytometry analysis of surface-bound Spike protein and its binding to hACE2 receptor.

Approximately 1×10^6 C2C12 mouse myoblast cells were prewashed in Opti-MEM low serum media (Gibco), electroporated (one pulse, 120 V, 25 ms) with SAM RNA (1 µg) and mouse thymus carrier RNA up to 4.2 µg total RNA (Takara). Cells were seeded in six-well plates with 1% FBS and P/S containing DMEM growth media and incubated at 37°C and 5% CO_2 for 18 hours. At 4 hours post transfection, Brefeldin A (BFA, BD Biosciences) was added to cells as needed following the manufacturer's recommendation. Cells were collected, washed, and stained with an anti-Spike antibody (1A9 mouse monoclonal IgG1, GeneTex) followed by a goat anti-mouse IgG Alexa 488 secondary antibody (Invitrogen). Cells were fixed with 1.5% paraformaldehyde in phosphate buffered saline (PBS) (Thermo Fisher), acquired on a Fortessa X20 SORP flow cytometer (BD Biosciences) and analyzed by FlowJo v10 software (BD Biosciences).

To assess the binding of hACE2 to Spike protein on the surface of SAM transfected cells, hACE2 recombinant protein was diluted 1:150 (0.31 mg/ml stock; Acro Biosystems) in PBS containing 2.5% FBS. Cells were spun down and incubated with the diluted hACE2 protein on ice for 30 minutes. Samples were washed and stained with a goat anti-hACE2 polyclonal antibody (R&D systems) followed by a rabbit anti-goat IgG Alexa 488 (Invitrogen). Cells were fixed with 1.5% paraformaldehyde in PBS, acquired on a Fortessa X20 SORP flow cytometer (BD Biosciences) and analyzed by FlowJo v10 software (BD Biosciences).

Human COVID-19 convalescent-phase serum (HCS) panel

Human samples were obtained with informed consent. All recruitment, sample collection, and experimental procedures using human samples have been approved by relevant institutional review boards and by GSK human sample management board. Human SARS-CoV-2 infection/COVID-19 convalescent sera (n=22) were drawn from donors 23-61 years of age, mostly from females, after PCR-confirmed diagnosis and at least 28 days after the participants were asymptomatic. Sera were obtained from CHU Tivoli, Belgium.

Ethical statement

All nonclinical studies were conducted in accordance with the GSK Policy on the Care, Welfare and Treatment of Laboratory Animals and were reviewed by the Institutional Animal Care and Use Committee by the ethical review process at the institution where the work was performed. All studies followed ARRIVE Guidelines as applicable and were conducted in compliance with provisions of the USDA Animal Welfare Act, the Public Health Service Policy on Humane Care and Use of Laboratory Animals and the U.S. Interagency Research Animal Committee Principles for the Utilization and Care of Research Animals.

MOUSE IMMUNOGENICITY STUDY

SARS-CoV-2 Spike-specific IgG binding antibody titers

The titers of Spike-specific IgG binding antibodies were measured using a Luminex-based assay (Luminex Corporation). The antigen used in this assay was a Spike ectodomain protein, encoding amino acid residues 1-1208 of Wuhan-Hu-1 strain (GenBank: MN908947) with proline substitutions at residues 986 and 987, a "GSAS" substitution at the furin cleavage site (residues 682–685), a C-terminal Foldon trimerization motif, a TEV protease cleavage site, a double StrepTag, and an 8x HisTag. The antigen sequence was synthesized, cloned into an in-house mammalian expression vector, similar in design to the one reported by Wrapp and co-authors, and produced and purified as previously reported.[16] Luminex microspheres were covalently coupled with the Spike protein using N-hydroxysulfosuccinimide and N-(3-dimethylaminopropyl)-N'-ethylcarbodiimide (EDC) according to the manufacturer's instructions. The microspheres were mixed with serial dilutions of mouse serum, incubated for 1 hour at room temperature (RT), washed with PBS, and suspended for 1 hour at RT in r-Phycoerythrin-conjugated anti-mouse IgG (Fcγ-specific, Jackson Immunoresearch) at a 1:50 dilution. The beads were then washed and resuspended in PBS. Fluorescence intensity was measured using a FlexMap 3D instrument (Luminex Corporation). A standard composed of a mix of 3 monoclonal antibodies to the Spike protein (anti-S2 1A9 mouse monoclonal IgG1 (GeneTex); anti-S2, mouse monoclonal IgG1 (MP Biomedical); anti-S1, human monoclonal IgG1 (Absolute Antibody)), diluted into naïve mouse serum, was assigned a value of 100 AU (Assay Units) and a standard curve of concentrations was plotted. Sample titers were interpolated on a 4-parameter logistic fit of the standard curve. Data points for calculation of sample titers were selected from within the range of 10% to 70% of the lower and upper asymptote of the standard

curve. The final sample titer was the average of the back calculated titers for dilutions falling within the acceptable range of the standard curve.

VSV-SARS-CoV-2 Spike pseudovirus neutralization assay

Neutralizing antibodies from HCS panel and immunized mice sera were assessed using a cell-based pseudovirus neutralization assay. A recombinant replication-deficient Vesicular stomatitis virus (VSV) vector that encodes a luciferase protein in place of VSV-G was pseudotyped with a Spike glycoprotein that lacked the last 19 amino acids of the cytoplasmic tail, derived from SARS-CoV-2 Wuhan, Alpha (B.1.1.7; HV 69-70 del, Y144 del, N501Y, A570D, D614G, P681H, T716I, S982A, D1118H mutations) or Beta (B.1.351; L18F, D80A, D215G, del242-244, R246I, K417N, N501Y, E484K, D614G, A701V mutations) variants or Delta (B.1.617.2; T19R, G142D, del156-157, R158G, L452R, T478K, D614G, P681R, D950N).[20]

Vero E6 cells expressing the hACE-2 receptor were seeded in 96-well white plates at 20,000 cells/well to reach a cell confluence of 80%. Serum samples or controls were diluted in duplicate in DMEM containing 10% FBS and P/S (growth media) at a starting dilution of 1/25, 1/250 or 1/2500 (for mouse samples), or 1/10, 1/100 or 1/1000 (for human samples), followed by a serial dilution (2-fold dilutions, 6 times). Pseudovirus was added to diluted serum samples and pre-incubated for 1 hour at 37°C with 5% CO_2. VSV-SARS-CoV-2 Spike pseudovirus diluted in cell growth media was used as the reference for 100% infectivity. The mixtures were then added to the pre-seeded Vero E6 cell layers and plates were incubated for 18-20 hours at 37°C with 5% CO_2. Media were removed, ONE-Glo EX Luciferase Assay Substrate (Promega) was added to cells, and incubated for 3 minutes at RT with shaking. Luminescence was measured using a microplate reader (SpectraMax i3x) and SoftMax Pro v6.5.1 (Molecular Devices). Luminescence results for each dilution were used to generate a titration curve using a 4-parameter logistic regression (4PL). Titers were established by determining the reciprocal of the serum dilution leading to a 50% reduction in signal compared to virus-only wells (pseudovirus 50% neutralization titers, $pVNT_{50}$). This was established using the 50% flanking points of the 4PL titration curve for each sample. The final titer was calculated as the average of replicates.

Live virus SARS-CoV-2 neutralization assay

A neutralization assay using a previously described strain of SARS-CoV-2 (isolate USA-WA1/2020), that had been rescued by reverse genetics and engineered by the insertion of a mNeonGreen (mNG) gene into open reading frame 7 of the viral genome, was used to measure neutralizing antibodies in the sera collected from mice 2 weeks after the second immunization.[19] Briefly, Vero CCL-81 cells (1.2×10^4) in DMEM containing 2% FBS and P/S were seeded in each well of a 96-well plate, and the cells were incubated overnight at 37°C and 5% CO_2. On the following day, serum samples were two-fold serially diluted in 2% FBS and P/S DMEM and incubated with mNG SARS-CoV-2 at 37°C for 1 hour. The virus-serum mixture was transferred to the Vero CCL-81 cell plate at a final multiplicity of infection (MOI) of 0.5. For each serum, the starting dilution was 1/20 with 9 two-fold dilutions to the final dilution of 1/5,120. After incubation for 16 hours at 37°C, 25 µl of Hoechst 33342 solution (400-fold diluted in Hank's Balanced Salt Solution, Gibco) was added to each well to stain the cell nucleus. The plate was sealed, incubated at 37°C for 20 minutes, and quantified for mNG fluorescence on CytationTM 7 (BioTek). The raw images were acquired using 4×objective and processed using the default setting. The total cells (indicated by nucleus staining) and mNG-positive cells were quantified for each well. Infection rates were determined by dividing the mNG-positive cell number by the total cell number. Relative infection rates were obtained by dividing the infection rates of serum-treated wells with the infection rate of the non-serum treated controls well. The curves of the relative infection rates versus the serum dilutions (log10 values) were plotted using Prism 8 (GraphPad). A nonlinear regression method was used to determine the dilution fold that neutralized 50% of mNG fluorescence (VNT50). Each serum was tested in duplicates. All mNG SARS-CoV-2 reporter neutralization assay was performed at the BSL-3 facility at University of Texas Medical Branch.

SARS-CoV-2 Spike-specific B cell responses in mice

Characterization of Spike-specific B cells from spleens and draining inguinal lymph nodes collected from immunized mice (2 independent experiments, 5 mice/group/experiment) at 2 weeks post the second immunization (2wp2) was performed using multi-parametric flow cytometry. Single cell suspensions prepared from spleen, or pairs of inguinal lymph nodes from each mouse, were stained with near-IR live/dead cell stain (Invitrogen) for 20 minutes

at RT, washed and incubated with mouse Fc block (BD Biosciences) in PBS plus 1% FBS (HyClone, Thermo Scientific) for 10 minutes at 4˚C. Approximately 1-2 $\times 10^6$ splenocytes or lymph node cells were stained for 30 minutes at 4˚C with the following commercial monoclonal antibodies: anti-CD3 (BUV737), anti-CD19 (BV786), anti-IgD (BV421), anti-IgM (BUV395), anti-GL7 (AF647), anti-CD95 (BV711), anti-CD138 (BB700), anti-CD38 (BV650), anti-CD80 (PECF594), anti-CD73 (PE-Cy7), and anti-CD273 (PE). All monoclonal antibodies were from BD Biosciences, except anti-CD73 PE-Cy7 which was from Biolegend. To identify Spike-specific B cells, samples were stained with 1 µg per 1-2 × 10^6 cells of SARS-CoV-2 Spike protein labelled with Alexa Fluor 488 (BD Biosciences) included in the antibody mix. Stained cells were analyzed on a FACSymphony A5 SORP cell analyzer (BD Biosciences). Data from two independent experiments were combined. Spike-specific B cells were identified within class-switched B cell population (identified as $CD3^-CD19^+IgM^-IgD^-$ B cells), which was further subdivided into memory B cells ($CD95^-CD38^+$), and germinal center B cells ($GL7^+CD95^+$). CD80, PD-L2 and CD73 markers were also used to provide further characterization of the Spike-specific B cells elicited by the SAM (LNP) vaccine.

Analysis of SARS-CoV-2 Spike-specific T cell responses in mice

Splenocytes were collected from mice at 2wp2 and SARS-CoV-2 Spike-specific T cell responses were assessed by intracellular cytokine staining and multi-parametric flow cytometry. Briefly, single cell suspensions of 1-2 $\times 10^6$ live splenocytes were plated in 96-well U-bottom plates (Corning) and incubated for 2 hours at 37ºC with 1 µg/ml of $Spike_{FL\text{-}2P}$ specific (Genscript), S1, S2 or RBD specific peptide pools (JPT Peptides) containing 15mer peptides overlapping by 11 amino acids or with cell culture medium (no peptide, for background subtraction) as control in complete RPMI and in the presence of anti-CD28 co-activation and anti-CD107a-PE degranulation markers (BD Biosciences). Golgi transport inhibitor BFA (BD Biosciences) at 1 µg/ml was added after 2 hours and the splenocytes incubated for an additional 12 hours at 37ºC. Cells were then stained with 1:1000 diluted near-IR LIVE/DEAD stain (Invitrogen) for 20 minutes at RT. Cells were subsequently washed, fixed and permeabilized with Cytofix/Cytoper (BD Biosciences) for 20 minutes at 4ºC, blocked with 1:15 diluted mouse Fc Block (anti-CD16/CD32) in 1X Perm/Wash Buffer (BD Biosciences) for 10 minutes at RT, and stained with antibody mix T cell surface markers (anti-CD3-BV711, anti-CD4-BUV395, anti-CD8-BUV805), activation marker (anti-CD44-PECF594), and intracellular cytokines (anti-Interferon (IFN)-γ-BV786, anti-Interleukin (IL)-2-APCR700, anti-Tumor Necrosis Factor (TNF)-α-BV650 (BD Biosciences), anti-IL-17F-A647 (Biolegend), anti-IL-4-FITC, anti-IL-13-FITC (eBiosciences)) in 1X Perm/Wash with Brilliant Stain Buffer (BD Biosciences) for 30 minutes at RT. All incubation steps after cell viability staining were conducted in the dark. Finally, the cells were washed and suspended in PBS plus 1% BSA (Gibco, Thermo Scientific), then acquired on BD FACSymphony A5 SORP cell analyzer and data were analyzed using FlowJo v10 software (BD Biosciences).

For analysis, cytokine responses (IFN-γ, TNF-α, IL-2, IL-4/IL-13, IL-17F,and CD107a) were measured on activated, $CD44^+$ T cell populations and subjected to Boolean analysis to yield 128 unique cytokine populations, including 64 unique populations for the $CD4^+$ compartment and 64 unique populations for the $CD8^+$ compartment. The IL-4 and IL-13 Th2 cytokines were assessed on the same FITC channel. The frequencies of each Boolean population were summed to yield the total cytokine response. The phenotype of T cell subsets was assessed as Th1 (defined as IFN-γ^+ IL-4^-IL-13^-; may or may not be IL-2^+, TNF-α^+, or $CD107a^+$), Th2 (defined as IL-4^+ and/or IL-13^+ and IFN-γ^-; may or may not be IL-2^+, TNF-α^+, or $CD107a^+$), Th17 (defined as IL-$17F^+$ and IFN-γ^-, IL-4^-IL-13^-; may or may not be IL-2^+, TNF-α^+, or $CD107a^+$), and Th0 (defined as IL-2^+ and/or TNF-α^+, and IFN-γ^-IL-$17F^+$IL-4^-IL-13^- ; may or may not be $CD107a^+$) for both $CD4^+$ (designated as Th0/Th1/Th2/Th17 T helper subsets) and $CD8^+$ (designated as Tc0/Tc1/Tc2/Tc17 T cytotoxic subsets) T cells. Additionally, polyfunctionality was assessed for selected vaccine groups using Pestle v2 and Simplified Presentation of Incredibly Complex Evaluations (SPICE v6.1) software (Joshua Nozzi & Mario Roederer; NIAID). The Spike-specific IL-17F and IL-4/IL-13 levels were negligible and thus excluded from polyfunctional SPICE analysis.

HAMSTER IMMUNOGENICITY AND EFFICACY STUDY

Plaque reduction neutralization test with hamster sera

Neutralizing antibodies in sera of vaccinated hamsters were determined by plaque reduction neutralization test as previously described.[47] Briefly, serum was heat-inactivated for 30 minutes at 56°C and diluted two-fold in BA-1 media starting at a 1:5 dilution on a 96-well plate. An equal volume of SARS-CoV-2 virus (isolate USA-WA1/2020; 100 PFU) was added to the serum dilutions and the sample-virus mixture was gently mixed. The plates were incubated

for 1 hour at 37°C. Following incubation, serum-virus mixtures were plated onto Vero plates. Antibody titers were recorded as the reciprocal of the highest dilution in which >90% of virus was neutralized. All hamsters were confirmed negative for the presence of antibodies against SARS-CoV-2 prior to vaccination.

Cytokine profiling in cultured hamster lung cells

Lungs were homogenized using syringe plunger and passed through a 70 µm filter to prepare single cell suspension. Erythrocytes were lysed by treating cells with Gey's RBC lysis buffer (0.15 M NH4Cl, 10 mM HCO3) for 2 minutes with constant shaking in between. After 2 minutes, complete media (RPMI-1640 with 10% FBS, 10% non-essential amino acids, 10% P/S and 10% L-Glutamine) was added to dilute the RBC lysis buffer. Cells were centrifuged at 500 x g for 10 minutes to pellet down cells and wash the pellet once with complete media. After washing, cells were suspended in 1mL complete media, homogenized and equal number of cells were added to each well in a U-bottom 96 well plate. Cells were cultured in 37°C CO_2 incubator without stimulation. After 24 hours the cultures were transferred into 96 well v-bottom plate, centrifuged at 500g for 7 minutes and supernatant was collected and transferred into 96 well flat bottom plates that were stored at -80°C until assay for cytokines. Supernatants were assayed for hamster IFN-γ, TNF-α, and IL-4 using competitive ELISA commercial kits (G Biosciences), following manufacturer's recommendations and provided standard curves to obtain cytokine concentrations.

Histopathology

Hamster tissues (trachea, lung, heart, liver, spleen, brain, kidney, adrenal glands, and thymus) were fixed in 10% neutral buffered formalin for at least 72 hours at RT prior to sectioning and slide preparation for standard Hematoxylin and Eosin (H&E)-stained sections. Additional sections of lung were stained with picrosirius red to evaluate the degree of pulmonary fibrosis. Tissue sections were evaluated by two board-certified veterinary pathologists and a consensus was agreed on all findings and interpretation. Key pathologic features were recorded as separate findings and graded on a 5-point scale (minimal, mild, moderate, marked, very marked/severe).

REPEATED-DOSE TOXICITY STUDY IN SPRAGUE-DAWLEY RATS

The welfare of the animals was maintained in accordance with the general principles outlined in the current Guidelines published by the Canadian Council on Animal Care and the Guide for the Care and Use of Laboratory Animals, a National Research Council Canada publication. The Institutional Animal Care and Use Committee (IACUC) at Citoxlab (now part of Charles River Laboratories, Inc) approved the study plans. The repeated dose toxicology and biodistribution studies were conducted in an Organization for Economic Cooperation and Development (OECD) member country and in accordance with the OECD Test Guidelines and the Principles of Good Laboratory Practice (GLP). The non-clinical development plan was defined in accordance with the World Health Organization (WHO) "Guidelines on Non-clinical Evaluation of Vaccines"[48] and the Food and Drug Administration (FDA) Guidance for Industry, "Considerations for Plasmid DNA Vaccines for Infectious Disease Indications".[49]

Clinical examinations

The animals were checked twice daily for mortality and signs of illness. Briefly, local skin reactions at the injection sites, such as erythema or edema, were recorded prior to dosing, and 6, 24, and 48 hours after each injection. The body weight of each animal was recorded once before group allocation, prior to first injection (Day −1), daily for 2 consecutive days following each injection and twice weekly until the next dose/study termination, including the day of necropsy. On each dosing occasion, rectal body temperature was measured for all surviving animals prior to vaccination and approximately 2, 4, 6, 12, 18, 24, and 48 hours post dosing. Ophthalmological examinations (funduscopy and biomicroscopy) were performed on all animals once during the pre-dosing period, after the last dosing occasion, and on recovery animals at the end of the recovery period.

Blood sampling, blood chemistry, hematology and serology

Hematology, coagulation and blood biochemistry investigations were performed at Days 2 (main animals), 8 (recovery animals), 30 (main animals), and 36 (recovery animals). Blood samples for the determination of anti-Spike IgG binding antibodies were collected from the jugular vein (non-terminal collection) of all animals before the

first vaccination (beginning of the treatment period) and from the abdominal aorta (under anesthesia with isoflurane) during necropsy (terminal collection) on Days 32 (main animals) and 57 (recovery animals). A Luminex-based antibody binding assay (Luminex Corporation) was used as described for mouse Spike-specific IgG binding antibody titers evaluation. A PE-conjugated anti-rat IgG (Fcγ-specific, Jackson Immunoresearch) at a 1:50 dilution was used for detection.

Necropsy, tissue processing and histopathological examination

At Days 32 and 57 (main and recovery animals, respectively), the rats were anesthetized by isoflurane and euthanized by exsanguination after blood collection. They were subjected to a detailed external (particularly the injection sites) and internal macroscopic examination for pathological changes. Adrenal glands, brain, draining lymph nodes (iliac, inguinal, popliteal), other lymph nodes (mandibular, mesenteric), epididymites, heart, kidneys, liver, lungs, ovaries, pituitary gland, prostate, spleen, testes, thymus, thyroids with parathyroid, and uterus were weighed and subsequently preserved in phosphate-buffered neutral 10% formaldehyde (except testes in Davidson's fixative) for microscopic evaluation. Other organs were preserved for examination, including aorta, cecum, colon, diaphragm, duodenum, esophagus, eyes and optic nerves (fixed in modified Davidson's fixative), femoral bone, Harderian glands, injection sites (muscle with skin and subcutis), ileum, jejunum (and Peyer's patches), lacrymal glands, larynx, nasal cavities, olfactory bulbs, rectum, salivary glands, oviducts, pancreas, sciatic nerve, seminal vesicles, triceps muscle, skin (with subcutis and mammary glands), spinal cord, sternum with bone marrow, stomach, tongue, trachea, ureters, urinary bladder, and vagina. Tissues intended for histological examination, according to a standard list of protocol designated tissues, were prepared by embedding in paraffin wax, sectioning and staining with hematoxylin and eosin. Briefly, representative tissue samples were fixed in 10% neutral buffered formalin, processed to slide and stained with H&E using routine histological methodology. Primary and peer-review pathology evaluation were both performed by board-certified pathologists. Any test article-related findings were graded on a standard, 5-point semiquantitative scale (minimal, mild, moderate, marked or severe).

Evaluation of tissue samples for biodistribution by RT-qPCR

After the determination of RNA concentration and verification of RNA integrity, samples were subjected to Reverse Transcription Quantitative Polymerase Chain Reaction (RT-qPCR). Extracted material was used as template for reverse transcription followed by PCR amplification with an RT-qPCR test carried out on a QuantStudio 5 Real-Time PCR System (Applied Biosystems). The primers and probes were designed to target a non-structural backbone region of the SAM construct. The sequence of the forward primer was 5′- GACGGACCGACAAGTCTCTA -3’; the sequence of the reverse primer was 5′- GGTGGTGTCAAAGCCTATCCA -3′, and the sequence of the internal Taqman probe was 5′- 6FAM - TCACCAAGC/ZEN/CAATAAGGGAGTT/IABkFQ-3'. An amount of 1 µg RNA in 5 µL was incubated with a 20 µL mix containing 5 µL TaqMan fast virus 1-step master mix (Thermofisher Scientific), 8.8 µL DNase/RNase-free water, 0.2 µM of each primer and 0.2 µM of hybridization probe. The amplification profile was 1 cycle of 5 minutes at 50°C (reverse transcription), one cycle of 20 seconds at 95°C (polymerase activation), and 40 cycles of 3 seconds at 95°C, followed by 30 seconds at 60°C (alternating denaturation and annealing/extension). Amplification was detected in real-time during the elongation step at 60°C by following the fluorescent signal generated by the degradation of the probe. The assay lower and upper limits of quantitation, limit of detection and inter- and intra-assay precision have been previously described.[40]